Swiss Permafrost Bulletin 2025

1 October 2024 to 30 September 2025

Annual report #7 on permafrost observations in the Swiss Alps

Swiss Permafrost Monitoring Network PERMOS

June 2026

Imprint

Publication of the Swiss Permafrost Monitoring Network (PERMOS).

Edited by

Jeannette Noetzli, PERMOS Office, WSL Institute for Snow and Avalanche Research SLF and Climate Change, Extremes and Natural Hazards in Alpine Regions Research Centre CERC, Davos Dorf

Cécile Pellet, PERMOS Office, Department of Geosciences, University of Fribourg, Fribourg

Data collection

The seven PERMOS Partner Institutions are responsible for the maintenance of the field installations and data collection at the PERMOS sites: ETH Zurich (ETHZ), Universities of Fribourg (UniFR), Innsbruck (UIBK), Lausanne (UniL) and Zurich (UZH), University of Applied Sciences and Arts of Southern Switzerland (SUPSI), and WSL Institute for Snow and Avalanche Research SLF (WSL-SLF).

Author contributions

Jeannette Noetzli, WSL-SLF: Sections 1, 2, 3, 6, 7
Cécile Pellet, UniFR: Sections 1, 4, 5, 7
Marcia Phillips, WSL-SLF: Section 6

Reviewed by

Members of the PERMOS Scientific Committee: Chantal Del Siro, Daniel Farinotti, Isabelle Gärtner-Roer, Tomasz Gluzinski, Christophe Lambiel, Coline Mollaret, Marcia Phillips, Cristian Scapozza, Samuel Weber.

Data availability

All PERMOS data are available online at https://www.permos.ch/data-portal and are subject to the PERMOS Data Policy (CC-BY 4.0). This report is based on the version 2026 of the PERMOS data set: https://doi.org/10.13093/permos-2026-01.

Citation

PERMOS 2026. Swiss Permafrost Bulletin 2025. Noetzli, J. and Pellet, C. (eds.). No. 7, 30 pp., doi.org/10.13093/permos-bull-26.

Cover page

Annual ERT measurement at the Schilthorn in the Bernese Oberland. Photo: C. Pellet

List of abbreviations

ALT	Active Layer Thickness
ECV	Essential Climate Variable
ERT	Electrical Resistivity Tomography
ETHZ	ETH Zurich
FOEN	Federal Office for the Environment
GCOS	Global Climate Observing System
GCW	Global Cryosphere Watch
GFI	Ground Freezing Index
GNSS	Global Navigation Satellite System
GTI	Ground Thawing Index
GTN-P	Global Terrestrial Network for Permafrost
GST	Ground Surface Temperature
MAAT	Mean Annual Air Temperature
MAGST	Mean Annual Ground Surface Temperature
rMAGST	running Mean Annual Ground Surface Temperature
MeteoSwiss	Federal Office of Meteorology and Climatology MeteoSwiss
PERMOS	Swiss Permafrost Monitoring Network
RGV	Rock Glacier Velocity
RSF	Rock Slope Failure
SCNAT	Swiss Academy of Sciences
SLF	WSL Institute for Snow and Avalanche Research SLF
SUPSI	University of Applied Sciences and Arts of Southern Switzerland
TGS	Terrestrial Geodetic Survey
UIBK	University of Innsbruck
UniFR	University of Fribourg
UNIL	University of Lausanne
UZH	University of Zurich

Summary

The Swiss Permafrost Monitoring Network PERMOS observes and documents the evolution of permafrost in the Swiss Alps as a coordinated national monitoring network since 2000 using field measurements of ground temperatures, electrical resistivity and rock glacier velocities.

The hydrological year 2025 – October 2024 to September 2025 – was the warmest in Switzerland above 1000 m asl. since measurements began in 1864. Mean annual surface air temperature was 1.53 °C above the 1991–2020 mean and 2.73 °C above the 1961–1990 mean. The hydrological year 2025 was further characterized by a very mild and snow-poor winter, a mild spring, and very warm atmospheric conditions during summer and autumn 2025.

As a result of the late onset of the snow cover and below-average snow heights throughout the winter, the mean annual ground surface temperatures (MAGST) were 0.1–2 °C lower in 2025 than in 2024 at the PERMOS sites, except for the steep bedrock sites. But in general, they remained above the 2012–2021 average. These surface conditions led to both lower and larger active layer thicknesses with changes compared to 2024 ranging from –0.5 to +0.5 m. Permafrost temperatures at 10 m and 20 m depth remained at high levels with new record temperatures registered at 70% of the boreholes.

The permafrost electrical resistivities measured in 2025 showed contrasting evolutions compared to 2024, with an increase of +26% at Stockhorn and a decrease of –3% and –1% at Lapires and Schilthorn. This reflects the different magnitude of cooling at the ground surface and is in line with the active layer and permafrost temperature reported at the sites.

Rock glacier velocity (RGV) decreased at most sites in 2025 compared to 2024. Over the Swiss Alps, RGV decreased by 13%, with regional changes ranging from –5% in the Lower Valais to –22% in the Engadine. This can be attributed to the stronger winter ground surface cooling.

In 2025, eight rock slope failures from permafrost areas were reported with estimated volumes between 1000 m^3 to 6 Mio m^3. All events had their starting zone in north-facing slopes in permafrost areas and occurred between May and October. The most striking event was the series of large rock slope failures from the snow-covered NE facing permafrost rock slopes on the Kleines Nesthorn above Blatten, which led to the deposition of 6 Mio m^3 on the Birchgletscher, provoking its failure.

Overall, the permafrost observations during the hydrological year 2025 point to very warm permafrost conditions close to record conditions, offset only by winter cooling at the ground surface due to the snow-poor winter. Active layer thickness, permafrost resistivity and rock glacier velocity show contrasting signals due to the different magnitude of ground surface cooling at the different sites.

Zusammenfassung

Das Schweizer Permafrost-Messnetz PERMOS beobachtet und dokumentiert seit dem Jahr 2000 als koordiniertes nationales Beobachtungsnetz die Entwicklung des Permafrosts in den Schweizer Alpen mittels Feldmessungen von Bodentemperaturen, elektrischem Widerstand und Geschwindigkeiten von Blockgletschern.

Das hydrologische Jahr 2025 – Oktober 2024 bis September 2025 – war in der Schweiz oberhalb von 1000 m ü. M. das wärmste seit Beginn der Messungen im Jahr 1864. Die mittlere jährliche Lufttemperatur lag 1.53 °C über dem Mittelwert von 1991–2020 und 2.73 °C über dem Mittelwert von 1961–1990. Das hydrologische Jahr 2025 war weiter geprägt durch einen sehr milden und schneearmen Winter, einen milden Frühling und sehr warme atmosphärische Bedingungen im Sommer und Herbst 2025.

Aufgrund des späten Einschneiens und der unterdurchschnittlichen Schneehöhen während des ganzen Winters lagen die mittleren jährlichen Bodenoberflächentemperaturen (MAGST) im Jahr 2025 an den PERMOS-Standorten um 0.1–2 °C unter jenen von 2024, mit Ausnahme der Standorte in steilem Fels. Im Allgemeinen waren sie jedoch weiterhin über dem Durchschnitt der Jahre 2012–2021. Diese Oberflächenbedingungen führten sowohl zu einer Zunahme wie auch Abnahme der Mächtigkeit der Auftauschicht im Bereich von –0.5 bis +0.5 m gegenüber dem Vorjahr. Die Permafrosttemperaturen in 10 m und 20 m Tiefe blieben auf hohem Niveau, wobei in 70% der Bohrlöcher neue Rekordtemperaturen verzeichnet wurden.

Die im Jahr 2025 gemessenen elektrischen Widerstände im Permafrost entwickelten sich gegensätzlich gegenüber 2024: sie nahmen am Stockhorn um 23% zu und an den Standorten Lapires und Schilthorn um 3% und 1% ab. Dies spiegelt die unterschiedlich starke Abkühlung an der Bodenoberfläche wider und entspricht auch den an diesen Standorten gemessenen Mächtigkeiten der Auftauschichten und Permafrosttemperaturen.

Die Blockgletscher-Geschwindigkeit (RGV) nahm 2025 an den meisten Standorten in den Schweizer Alpen im Vergleich zu 2024 ab und sank um 13 %. Regionale Änderungen zum Vorjahr reichten von –5 % im Unterwallis zu –22 % im Engadin. Dies steht im Zusammenhang mit der stärkeren Abkühlung der Bodenoberfläche im Winter.

Im Jahr 2025 wurden acht Felssturzereignisse aus Permafrostgebiet mit geschätzten Volumina von 1000 m³ bis zu 6 Mio. m³ dokumentiert. Alle Ereignisse starteten aus Nordhängen in Permafrostgebieten und ereigneten sich zwischen Mai und Oktober. Das grösste Ereignis war die Serie grosser Felsstürze von den schneebedeckten Nordost-Permafrost-Felshängen am Kleinen Nesthorn oberhalb von Blatten (VS), die 6 Mio. m³ Material auf dem Birchgletscher ablagerten und schliesslich dessen Abbruch auslösten.

Insgesamt zeigen die Permafrostbeobachtungen im hydrologischen Jahr 2025 sehr warme Permafrostbedingungen, die nahe an Rekordwerten lagen und nur durch die winterliche Abkühlung an der Bodenoberfläche aufgrund des schneearmen Winters etwas gemildert wurden. Die Mächtigkeit der Auftauschicht, der elektrische Widerstand im Permafrost und die Blockgletscher-Geschwindigkeit zeigten aufgrund des unterschiedlich starken Abkühlung an der Bodenoberfläche an verschiedenen Standorten gegensätzliche Signale für das Beobachtungsjahr.

Résumé

Le réseau suisse d'observation du pergélisol PERMOS documente en tant que réseau national coordonné, l'évolution du pergélisol dans les Alpes suisses depuis l'an 2000, à l'aide de mesures sur le terrain de la température du sol, de la résistivité électrique et de la vitesse des glaciers rocheux.

En suisse, l'année hydrologique 2025 (d'octobre 2024 à septembre 2025) a été, au-dessus de 1000 m d'altitude, l'année la plus chaude depuis le début des mesures en 1864. La moyenne annuelle des températures de l'air a dépassé de 1.53 °C la moyenne de la période 1991–2020 et de 2.73°C celle de la période 1961–1990. L'année hydrologique 2025 a en outre été marquée par un hiver 2024/2025 très doux et peu enneigé, un printemps doux, ainsi que des conditions atmosphériques très chaudes durant l'été et l'automne.

En raison du développement tardif du manteau neigeux et d'une hauteur de neige inférieure à la moyenne tout au long de l'hiver, la moyenne annuelle des températures à la surface du sol a été de 0.1 à 2°C plus basse en 2025 qu'en 2024 sur tous les sites PERMOS, à l'exception des parois rocheuses. De manière générale, les valeurs sont toutefois restées supérieures à la moyenne de la période 2012–2021. Ces conditions de surface ont entraîné à la fois une diminution et une augmentation de l'épaisseur de la couche active, avec des variations par rapport à 2024 comprises entre –0.5 et +0.5 m. Les températures du pergélisol à 10 m et 20 m de profondeur sont restées à des niveaux élevés et de nouveaux records ont été enregistrés dans 70% des forages.

Les résistivités électriques mesurées dans le pergélisol en 2025 ont évolué de façon contrastée par rapport à 2024, avec une augmentation de +26% à Stockhorn et une baisse de –3% et –1% respectivement à Lapires et au Schilthorn. Cela reflète les différences d'amplitude du refroidissement à la surface du sol et concorde avec l'épaisseur de la couche active et les températures du pergélisol relevées sur ces sites.

En 2025 la vitesse des glaciers rocheux a diminué sur la plupart des sites par rapport à 2024. Dans l'ensemble des Alpes suisses, elle a baissé de 13% en moyenne, avec des variations régionales allant de –5% dans le Bas-Valais à –22% en Engadine. Ce constat peut être attribué au refroidissement plus ou moins marqué de la surface du sol en hiver suivant les régions.

Huit éboulements provenant de zones de pergélisol ont été signalés en 2025, avec des volumes estimés entre 1000 m^3 et 6 millions de m^3. Les zones de déclanchement de tous ces événements se situaient sur des versants nord en zone de pergélisol. Ils ont eu lieu entre mai et octobre. L'événement le plus marquant a été la série de larges éboulements qui est survenue sur le versant nord-est du Kleines Nesthorn au-dessus de Blatten et qui a déposé 6 millions de m^3 sur le Birchgletscher, provoquant ainsi sa rupture.

Dans l'ensemble, les observations du pergélisol au cours de l'année hydrologique 2025 indiquent des conditions de pergélisol très chaudes, proches des records historiques, compensées uniquement par un refroidissement hivernal à la surface du sol dû à une faible quantité de neige. L'épaisseur de la couche active, la résistivité du pergélisol et la vitesse des glaciers rocheux présentent des signaux contrastés en raison de l'ampleur variable du refroidissement à la surface du sol entre les différents sites.

Riassunto

La Rete Svizzera di Osservazione del Permafrost PERMOS misura e documenta l'evoluzione del permafrost nelle Alpi svizzere dal 2000 quale rete nazionale di monitoraggio coordinato, avvalendosi di misurazioni sul terreno della temperatura del suolo, della resistività elettrica e della velocità dei ghiacciai rocciosi.

L'anno idrologico 2025 (ottobre 2024 a settembre 2025) ed è stato il più caldo mai registrato in Svizzera al di sopra dei 1000 m s.l.m. dall'inizio delle misurazioni nel 1864. La temperatura media annua dell'aria in superficie è stata di 1.53 °C superiore alla norma 1991–2020 e di 2.73 °C superiore alla norma 1961–1990. L'anno idrologico 2025 è stato inoltre caratterizzato da un inverno molto mite e povero di neve, da una primavera mite e da condizioni atmosferiche molto calde durante l'estate e l'autunno 2025.

A causa del ritardo nello sviluppo della copertura nevosa e delle altezze di neve inferiori alla media registrate durante tutto l'inverno, le temperature medie annue della superficie del suolo (MAGST) sono risultate inferiori di 0.1–2.0 °C rispetto al 2024 nei siti PERMOS, a eccezione di quelli situati nelle pareti rocciose, pur rimanendo generalmente più elevate della media 2012–2021. Queste condizioni di superficie hanno causato degli spessori dello strato attivo sia inferiori sia superiori rispetto al 2024, con variazioni comprese fra –0.5 e +0.5 m. Le temperature del permafrost a 10 e 20 m di profondità sono rimaste a livelli elevati, con nuove temperature record registrate rispettivamente in 17 e 13 perforazioni.

Le resistività elettriche del permafrost misurate nel 2025 hanno mostrato andamenti contrastanti rispetto al 2024, con un aumento del +26% allo Stockhorn e una diminuzione del –3% ai Lapires e del –1% allo Schilthorn. Ciò riflette la diversa magnitudo del raffreddamento alla superficie del suolo ed è in linea con le temperature dello strato attivo e del permafrost registrate in questi siti.

Nel 2025 la velocità dei ghiacciai rocciosi (RGV) è diminuita nella maggior parte dei siti rispetto al 2024. Nelle Alpi svizzere, RGV è diminuita del 13%, con variazioni regionali comprese fra il –5% del Basso Vallese e il –22% dell'Engadina. Ciò può essere attribuito al più intenso raffreddamento invernale della superficie del suolo.

Otto frane di crollo in roccia originatesi in aree di permafrost sono state segnalate nel 2025, con volumi stimati compresi fra 1000 m^3 e 6 Mio m^3. Tutti gli eventi si sono innescati in versanti esposti a nord in aree di permafrost e sono avvenuti tra maggio e ottobre. L'evento più eclatante è stato la successione di grandi frane di crollo generatesi dal versante roccioso nord-est del Kleines Nesthorn sopra a Blatten, caratterizzato da permafrost e ancora coperto di neve, che ha generato un accumulo di 6 Mio m^3 di detriti sul Birchgletscher, provocandone il collasso e la successiva distruzione del villaggio sottostante.

Nel complesso, le osservazioni del permafrost compiute durante l'anno idrologico 2025 indicano delle condizioni di permafrost molto calde e vicine ai livelli record, compensate solo dal raffreddamento invernale della superficie del suolo dovuto allo scarso innevamento. Lo spessore dello strato attivo, la resistività del permafrost e la velocità dei ghiacciai rocciosi mostrano segnali contrastanti a causa della diversa magnitudo del raffreddamento della superficie del suolo nei vari siti studiati.

Contents

1 Introduction

The Swiss Permafrost Monitoring Network (PERMOS, www.permos.ch) is the coordinated national network for systematically monitoring the evolution of mountain permafrost in the Swiss Alps, based on field measurements of selected permafrost core variables. PERMOS was established in 2000, and results have been summarized annually in the *Swiss Permafrost Bulletin* since 2019. Annual reporting is based on hydrological years because the snow cover strongly influences permafrost conditions. This bulletin documents the results of permafrost observations for the hydrological year 2025, covering the period from 1 October 2024 to 30 September 2025.

Permafrost is a key component of the cryosphere and is defined as ground that remains at or below 0 °C for at least two consecutive years. In the Swiss Alps, it typically occurs above ca. 2200 m asl and underlies 3–5% of the Swiss territory. Permafrost exists hidden in bedrock and rock debris slopes in high mountain areas. It is sensitive to changing atmospheric conditions and is recognized by the Global Climate Observing System (GCOS) of the World Meteorological Organization (WMO) as an Essential Climate Variable (ECV). Three key variables – referred to as ECV quantities – have been defined for global permafrost monitoring: permafrost temperature, active layer thickness and rock glacier velocity (WMO 2022; Irrgang et al. 2024). Internationally, permafrost observations are coordinated by the Global Terrestrial Network for Permafrost (GTN-P) (Streletskiy et al. 2021).

The PERMOS monitoring strategy is based on field measurements of three permafrost core variables, aligning with and complementing the quantities of the ECV permafrost (Figure 1.1):

1) **Ground temperature** near the surface and at depth,
2) **Permafrost electrical resistivity**, and
3) **Rock glacier velocity** (RGV).

Direct observation of permafrost is achieved through continuous ground temperature measurements at multiple depths in boreholes extending to depths of 100 m (Noetzli et al. 2021; Irrgang et al. 2024). These point measurements are supplemented by spatially distributed recordings of ground surface temperature. Changes in the ground ice and water content are assessed using permanently installed geoelectrical profiles at borehole sites (Mollaret et al. 2019). RGV is determined using annual terrestrial geodetic surveys (Roer et al. 2008; Irrgang et al. 2024; Kellerer-Pirklbauer et al. 2026) and permanently installed GNSS devices. The active layer thickness (ALT) – the thickness of the seasonally

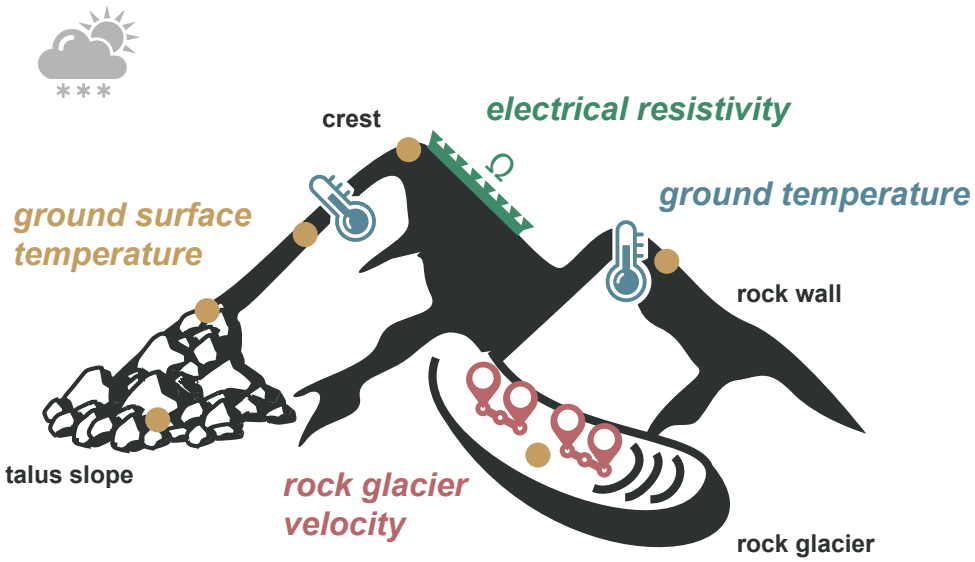

Figure 1.1. The PERMOS monitoring strategy includes the permafrost core variables ground temperature near the surface and at depth, permafrost electrical resistivity, and rock glacier velocity. The main permafrost landforms observed are indicated in black.

thawed layer above the permafrost – is derived from continuous ground temperature time series measured at multiple depth. It is defined as the deepest seasonal penetration of the 0 °C isotherm.

The following data are additionally collected to complement the set of permafrost core variables:

4) **Meteorological data** with automatic weather stations at selected borehole sites, and
5) **Rock Slope Failure (RSF)** events originating in permafrost areas in a database.

In 2025, the PERMOS network comprised 27 field sites (Figure 1.2, Table 1.1). Ground surface temperature (GST) was measured at 222 locations at 21 sites. Ground temperatures were recorded in 23 boreholes with depths ranging from 14 to 100 m at 14 sites, six of which were equipped with automatic weather stations. Geophysical surveys were conducted annually along permanently installed profiles at five borehole sites. RGV was measured at 15 sites on 18 rock glaciers using annual terrestrial surveys, and eight rock glaciers were equipped with permanent GNSS devices for continuous monitoring.

The selection of field sites for long-term permafrost observation follows landform-based approach, as permafrost change patterns related to topography, snow regime, and ground ice content are considered more important than regional climatic differences (PERMOS 2019; Noetzli et al. 2024). Most PERMOS sites were originally established in the framework of research projects and have been maintained by partner institutions for several decades. The monitoring strategy and site network are regularly reviewed and adapted based on relevance, technological advances, research findings, and operational feasibility.

Seven partner institutions are responsible for instrument maintenance and data collection at PERMOS sites: ETH Zurich, Universities of Fribourg (UniFR), Innsbruck (UIBK), Lausanne (UNIL) and Zurich (UZH), University of Applied Sciences and Arts of Southern Switzerland (SUPSI), and the WSL Institute for Snow and Avalanche Research SLF (SLF).

The PERMOS Office, jointly operated by SLF and UniFR, manages the network, implements the monitoring strategy, curates the data, and reports the results. PERMOS is financially supported by the

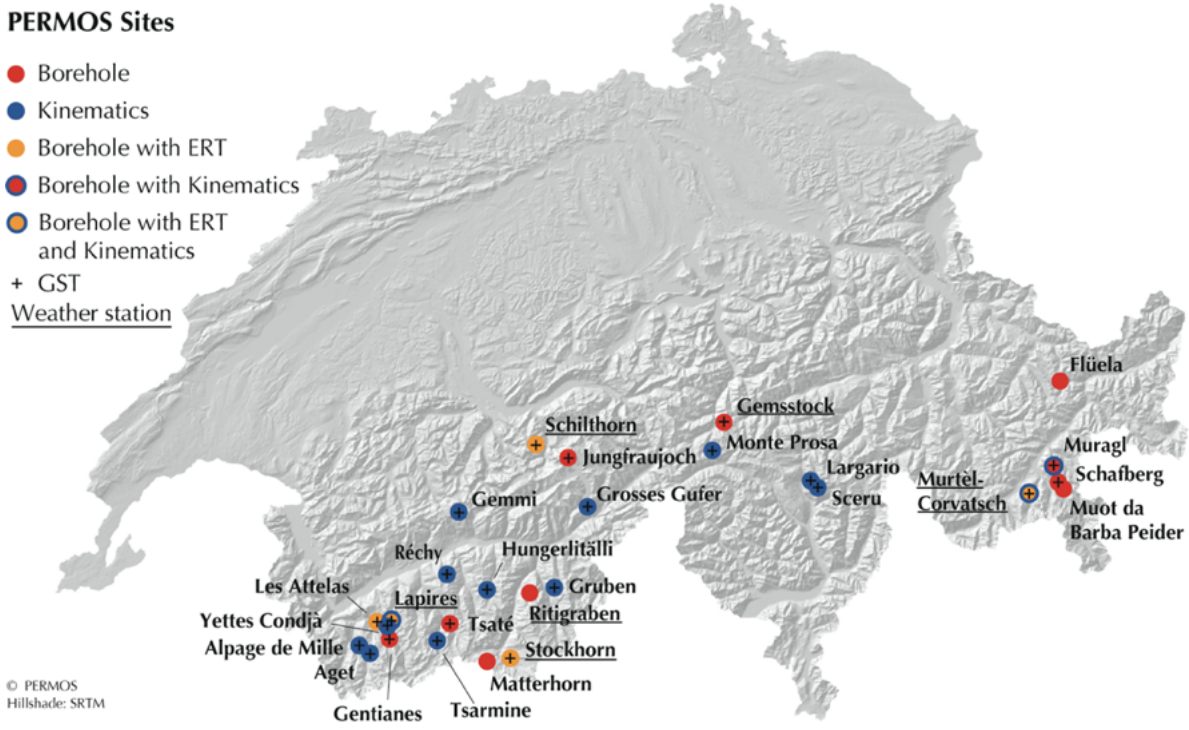

Figure 1.2. PERMOS field sites and applied methods.

Federal Office of Meteorology and Climatology MeteoSwiss in the framework of GCOS Switzerland, the Swiss Federal Office for the Environment (FOEN) and the Swiss Academy for Sciences (SCNAT). Two standing committees provide oversight: the PERMOS Steering Committee, which advises on strategic and financial matters (PERMOS Steering Committee), and the PERMOS Scientific Committee, which provides scientific guidance.

Table 1.1. Location and characteristics of the PERMOS sites and type of variable measured at the site: BHT is borehole temperature (ground temperature measured in boreholes), GST is ground surface temperature, ERT is Electrical Resistivity Tomography, TGS is Terrestrial Geodetic Survey and GNSS are permanent GNSS devices. X and Y denote CH1903+ coordinates, and Z is the elevation in m asl. Coordinates indicate the general location of a site.

Name	Abb.	Region	Morphology	X	Y	Z	BHT	GST	ERT	TGS	GNSS	Meteo
Aget	AGE	Lower Valais	rock glacier	2584500	1095300	2800		X		X		
Les Attelas	ATT	Lower Valais	talus slope	2587200	1105000	2700	X	X	X			
Flüela	FLU	Engadine	talus slope, rock glacier	2791500	1180500	2400	X					
Gemsstock	GEM	Urner Alps	crest	2689800	1161800	2900	X	X				X
Gentianes	GEN	Lower Valais	moraine	2589400	1103600	2900	X	X				
Gemmi	GFU	Upper Valais	rock glacier, solifl. lobe	2614800	1139500	2750		X		X	X	
Grosses Gufer	GGU	Upper Valais	rock glacier	2649350	1141900	2400		X		X	X	
Gruben	GRU	Upper Valais	rock glacier	2640500	1113500	2800		X		X	X	
Hungerlitaelli	HUT	Upper Valais	rock glaciers	2621500	1115500	3000		X		X		
Jungfraujoch	JFJ	Bern. Oberland	crest	2641000	1155100	3700	X					
Lapires	LAP	Lower Valais	rock glacier, talus slope	2588070	1106080	2700	X	X	X	X		X
Stabbio di Largario	LAR	Ticino	rock glacier	2719000	1148500	2550		X		X	X	
Matterhorn	MAT	Upper Valais	crest	2618400	1092300	3200	X					
M. d Barba Peider	MBP	Engadine	talus slope	2791300	1152500	2950	X					
Alpage de Mille	MIL	Lower Valais	rock glacier	2581800	1096800	2500		X		X		
Monte Prosa	MPR	Ticino	rock glacier	2687450	1157700	2500		X		X	X	
Muragl	MUR	Engadine	rock glacier	2791000	1153700	2600	X	X		X	X	
Murtèl-Corvatsch	COR	Engadine	rock glacier, talus slope	2783150	1144700	2650	X	X	X	X	X	X
Réchy	REC	Lower Valais	rock glacier	2605900	1113300	3100		X		X	X	
Ritigraben	RIT	Upper Valais	rock glacier	2631700	1113700	2600	X					X
Schafberg	SBE	Engadine	rock glacier	2790900	1152700	2700	X	X				
Valle di Sceru	SCE	Ticino	rock glacier, talus slope	2720200	1145600	2500		X		X		
Schilthorn	SCH	Bern. Oberland	crest	2630400	1156400	2900	X	X	X			X
Stockhorn	STO	Upper Valais	crest	2629850	1092850	3400	X	X	X			X
Tsarmine	TMI	Lower Valais	rock glacier	2605300	1099400	2500		X		X		
Tsaté	TSA	Lower Valais	crest	2608500	1106400	3000	X	X				
Yettes Condjà	YET	Lower Valais	rock glacier	2588300	1105000	2700		X		X		

2 Weather and climate

2.1 Background

Surface air temperature (SAT) and snow depth are the key meteorological variables controlling seasonal variability and the long-term evolution of the ground thermal regime. Changes in SAT directly influence ground surface temperatures (GST) during periods with little or no snow, and throughout the year at locations where a thick winter snow cover cannot form, such as near-vertical bedrock slopes or wind-exposed ridges.

A thick winter snow cover insulates the ground from atmospheric conditions. The timing of snow onset in early winter and snowmelt in spring is therefore critical for the ground thermal regime. An early snow cover preserves heat in the ground from summer and autumn, whereas a long-lasting snow cover insulates the ground from atmospheric warming in spring and early summer. Conversely, late snow onset allows stronger ground cooling in early winter, while early snowmelt can lead to earlier ground warming in spring.

The weather and climate information provided below is based on MeteoSwiss (2025, 2026) and Haberkorn et al. (2025).

2.2 Conditions in 2025

The hydrological year 2025 started with the 9th mildest autumn since the start of the measurements in 1864 and with SAT 0.8 °C above the mean long-term reference period 1991–2020 (Figure 2.1). October 2024 was rainy, particularly in Valais and in the South, while the first part of November 2024 was sunny and warm. Some stations at higher elevations even recorded the warmest November. In the last third of the month, winter started in the high mountains with heavy snow falls. December, January and February were mild, and particularly at higher elevations February was very warm with +2 °C compared to the mean 1991–2020. Snow fell mainly in December and January and mainly in the South and West, followed by a dry February when only 10% of the average precipitation was recorded in parts of Grisons and the Valais. This resulted in below average snow heights from December 2024 to February 2025, particularly in the eastern part of the country, which is a contrast to the large snow heights in the previous winter. In the first half of March and at the end of Spring, large snow falls occurred in the South with more than 1 m of snow above 1800 m asl.

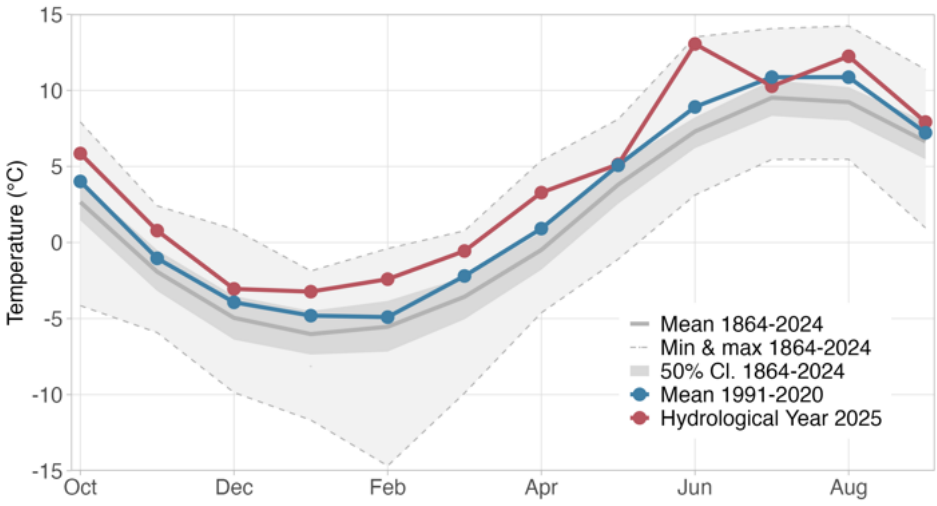

Figure 2.1. Monthly mean air temperatures of the hydrological year 2025 (October 2024 to September 2025) compared to previous measurements since 1864 and the mean of the most recent reference period 1991–2020. Data source: MeteoSwiss, homogenized data series for Swiss stations above 1000 m asl.

Overall, the winter of 2024/25 was in the top ten of the mildest winters since 1864 and characterised by well below-average snow heights, mainly due to low precipitation throughout Switzerland (Figure 2.2). The largest snow deficit was observed in northern and central Grisons with only 29% of the snow heights compared to the long-term mean 1991–2020. The smallest snow deficit at the end of winter 2025 was observed south of the main Alpine ridge, at 42% of the long-term mean 1991–2020. All over Switzerland, 36% of the normal snowfall was recorded at 2000 m in mid-April 2025.

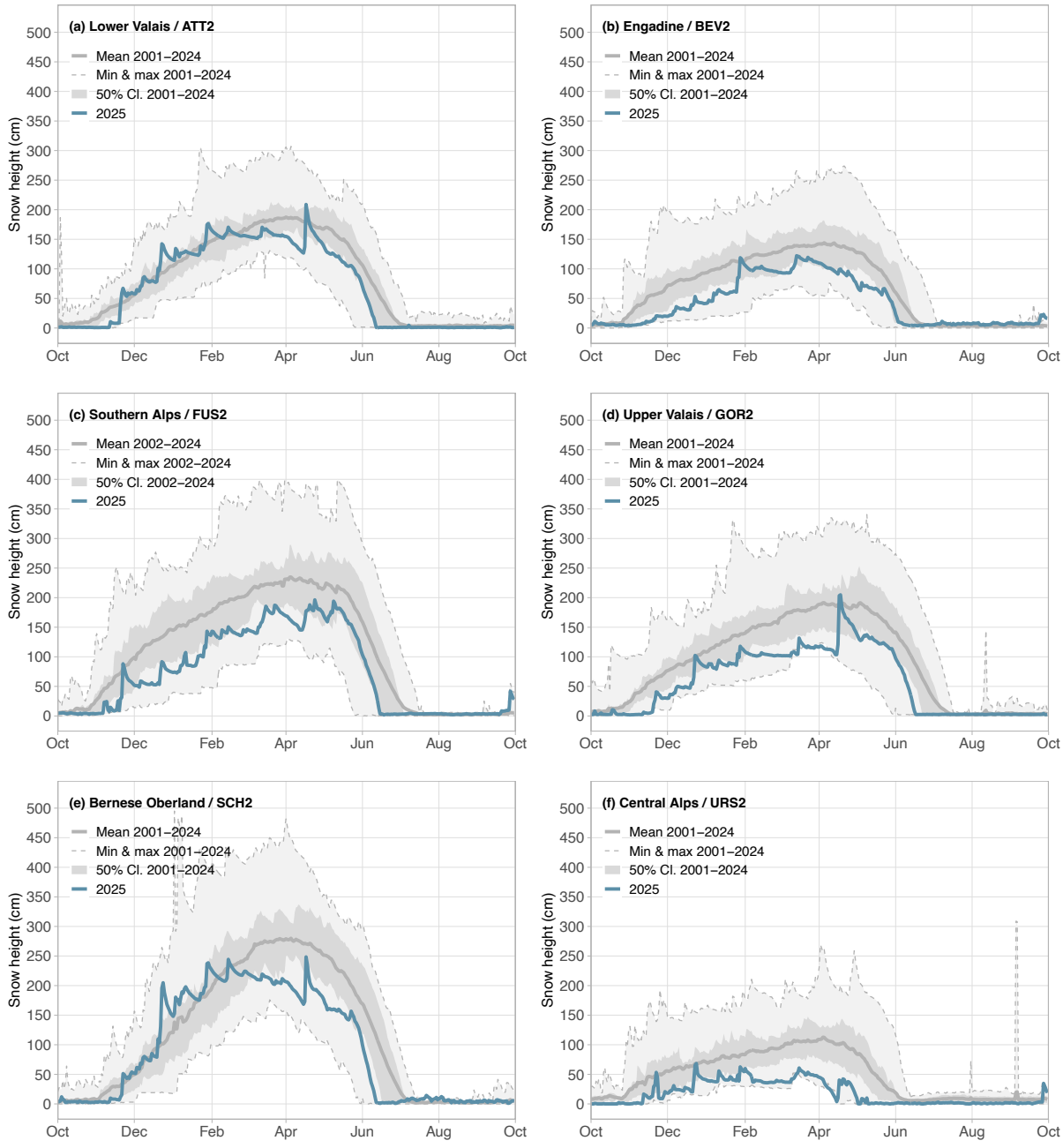

Figure 2.2. Snow height at six IMIS weather stations during winter 2025 compared to the mean, 25th and 75th percentiles of the period 2001–2024. Data were corrected for outliers and aggregated to daily median values. The stations represent different regions in the Swiss Alps: a) Lower Valais, b) Engadine, c) Southern Alps, d) Upper Valais, e) Bernese Oberland, and f) Central Alps. Data source: IMIS/SLF.

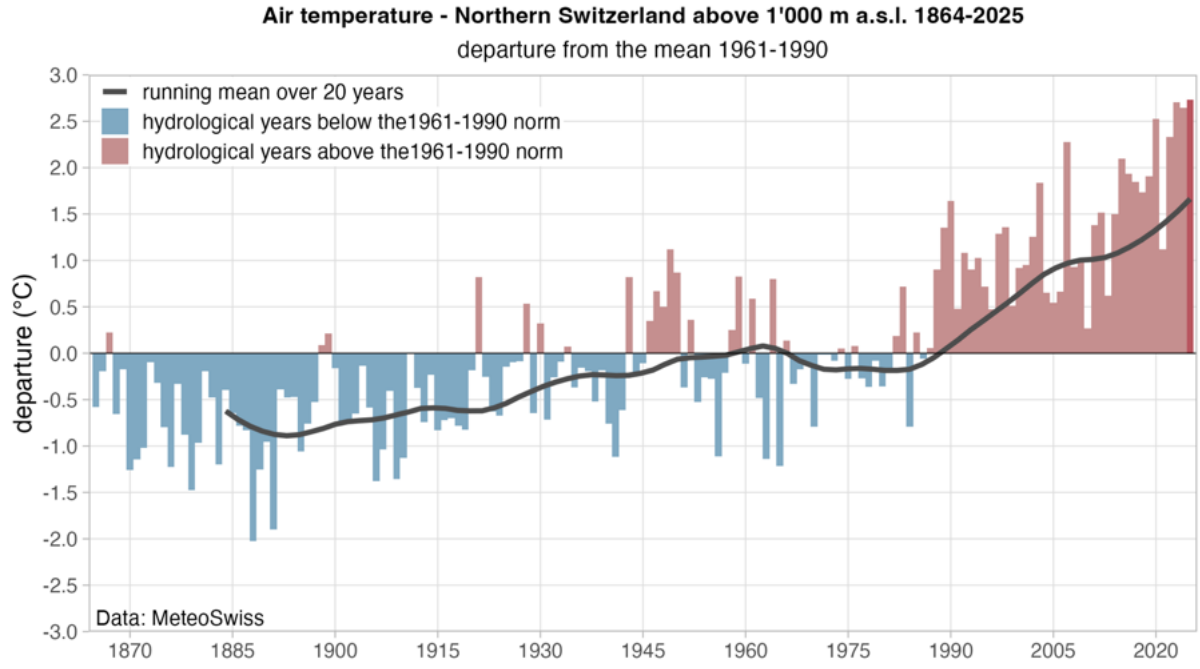

Figure 2.3. Annual air temperature deviation from the 1961–1990 climate norm based on homogenized data series for Swiss stations above 1000 m asl. for 1864–2025. Annual values refer hydrological years (October to September). The darker red color of the rightmost bar highlights the reporting year. Adapted from MeteoSwiss, data source: MeteoSwiss.

Spring 2025 was rather dry and the fourth warmest recorded since 1864 above 1000 m asl with 1.4 °C above the long-term average. This is comparable to spring 2020 and 2022. Sommer 2025 was one of the seven warmest since the begin of measurements and 1.6 °C above the long-term mean. The hot months June and August were interrupted by a wet and cold July. June was the second warmest and it was particularly warm at higher elevations. For example, it was even the warmest June ever recorded on Jungfraujoch. September 2025 was average warm and below average wet.

In summary, the hydrological year 2025 was characterized by a very mild and snow-poor winter, a mild spring, and very warm atmospheric conditions during summer and autumn (Figure 2.1). It was the warmest hydrological year in Switzerland above 1000 m asl. since measurements began in 1864 (Figure 2.3). The calendar year 2025 was 4th warmest on record, following 2022–2024. SAT was 1.53 °C above the reference period 1991–2020 and 2.73 °C above the 30-year average for 1961–1990, the WMO reference period for long-term climate monitoring (Figure 2.3).

3 Ground temperatures and active layer thickness

3.1 Background

Ground temperatures provide direct, quantitative, and comparable observations of the permafrost thermal state and are continuously measured at multiple depths in boreholes (Section 3.3). Borehole observations are complemented by spatially distributed ground surface temperature (GST) measurements (Section 3.1). Ground temperature measurements in permafrost are also used to determine the active layer thickness (ALT), defined as the maximum thickness of the uppermost ground layer that thaws each summer (Section 3.2).

Ground surface temperatures

GST reflect meteorological conditions during snow-free periods. The thermal conditions at the ground surface result from the energy balance and are predominantly influenced by solar radiation and SAT during snow-free periods (e.g., Hoelzle et al. 2022). Changes in ground temperature and the permafrost are primarily driven by changes in GST, which penetrate deeper into the ground with increasing delay and attenuation. Spatially distributed measurements at ca. 10 cm depth allow assessment of spatial GST variability related to topography and surface characteristics.

Active Layer Thickness

The ALT is defined as the maximum depth reached by the 0 °C isotherm during summer or autumn. The base of the active layer corresponds to the permafrost table, with the permafrost body lying below. Inter-annual variations in ALT are influenced by varying thermal conditions at the ground surface and in the uppermost metres as well as by the ground ice content. ALT variations in ice-rich ground are smaller than in ice-poor bedrock due to latent heat effects: the energy absorbed or released during phase change buffers temperature fluctuations, reducing the impact of unusually warm years on ALT.

Permafrost temperatures

In the uppermost metres below the surface, ground temperatures react to short-term GST variations. At 10 m depth, only larger seasonal variations are reflected, with a lag of about half a year. Below the so-called depth of the zero annual amplitude (DZAA), seasonal variations fall below 0.1 °C. In the Swiss Alps, DZAA is typically at around 15–20 m. At depths below the DZAA, ground temperatures respond to multi-annual atmospheric changes with delays of years (around 20 m depth) to decades (> ca. 50 m depth).

3.2 Ground surface temperatures

GST are continuously recorded using miniature temperature data loggers placed near boreholes, along geophysical profiles and next to geodetic survey points. At each site, 5–16 loggers are distributed to capture the spatial variability related to topography (elevation, slope and aspect) and surface conditions (debris and snow cover). Recording intervals are typically 1–3 hours, depending on the device type (storage capacity). Loggers are buried at around 10 cm depth to shield them from direct solar radiation, which could warm the casing. Data are read out annually on site at the end of the hydrological year.

Postprocessing of individual GST time series includes validity checks, aggregation to daily mean values and subsequent gap-filling using the quantile mapping approach described by Staub et al. (2017). To calculate site means daily time series, gaps were filled up to 3 years and only the longest

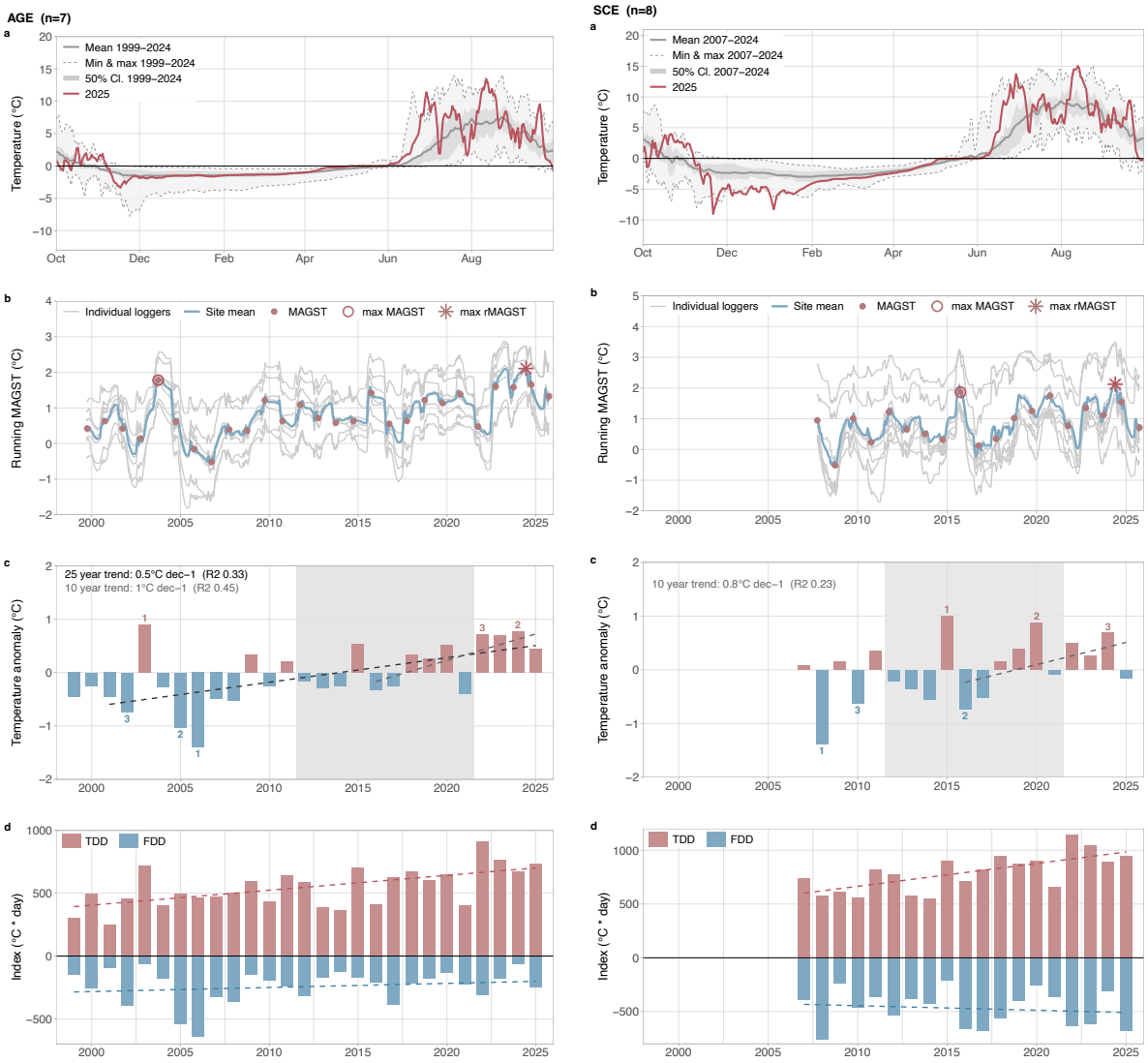

Figure 3.1. Ground surface temperatures at two rock glacier sites in the Lower Valais and in Ticino with long and complete time series: Aget (AGE, left) and Sceru (SCE, right). a) Daily mean GST at the sites during the hydrological year 2025 compared to all previous years. b) Running annual mean (rMAGST, thick blue line). The mean annual ground surface temperature (MAGST) is shown with orange dots, the maximum MAGST of the time series with a circle, and the maximum rMAGST with an asterisk. c) Departure of the MAGST from the 2012–2021 decadal mean. Linear trends for the last one and two decades are shown with dashed lines. d) Ground thawing and freezing indexes with linear trend lines.

and complete time series were selected. The resulting GST data set 2025 includes 222 time series from 21 sites with 1–14 time series per site (at some sites, time series are divided into different groups for reporting, resulting in 28 report groups). At several sites, GST data are assigned to different reporting groups to account for different terrain characteristics (e.g. in snow-influenced terrain or steep terrain without snow cover in winter, on bedrock or in coarse blocks, etc.). Data from 6 reporting groups at 5 sites are not included in the analyses for the hydrological year 2025 because they do not cover the reporting period (at GFU data only cover summer 2025 whilst at COR_W, COR_R, HUT, MPR, and TSA data were not collected in 2025). Daily GST was further aggregated to monthly and annual means following the completeness criteria for SAT by WMO (2017).

Following the very warm ground surface conditions and widespread record values of mean annual ground surface temperatures (MAGST) observed in 2024, MAGST for the hydrological year 2025 was 0.1–2 °C lower than in the previous year at all sites but one (Figure 3.1). At the same time, however,

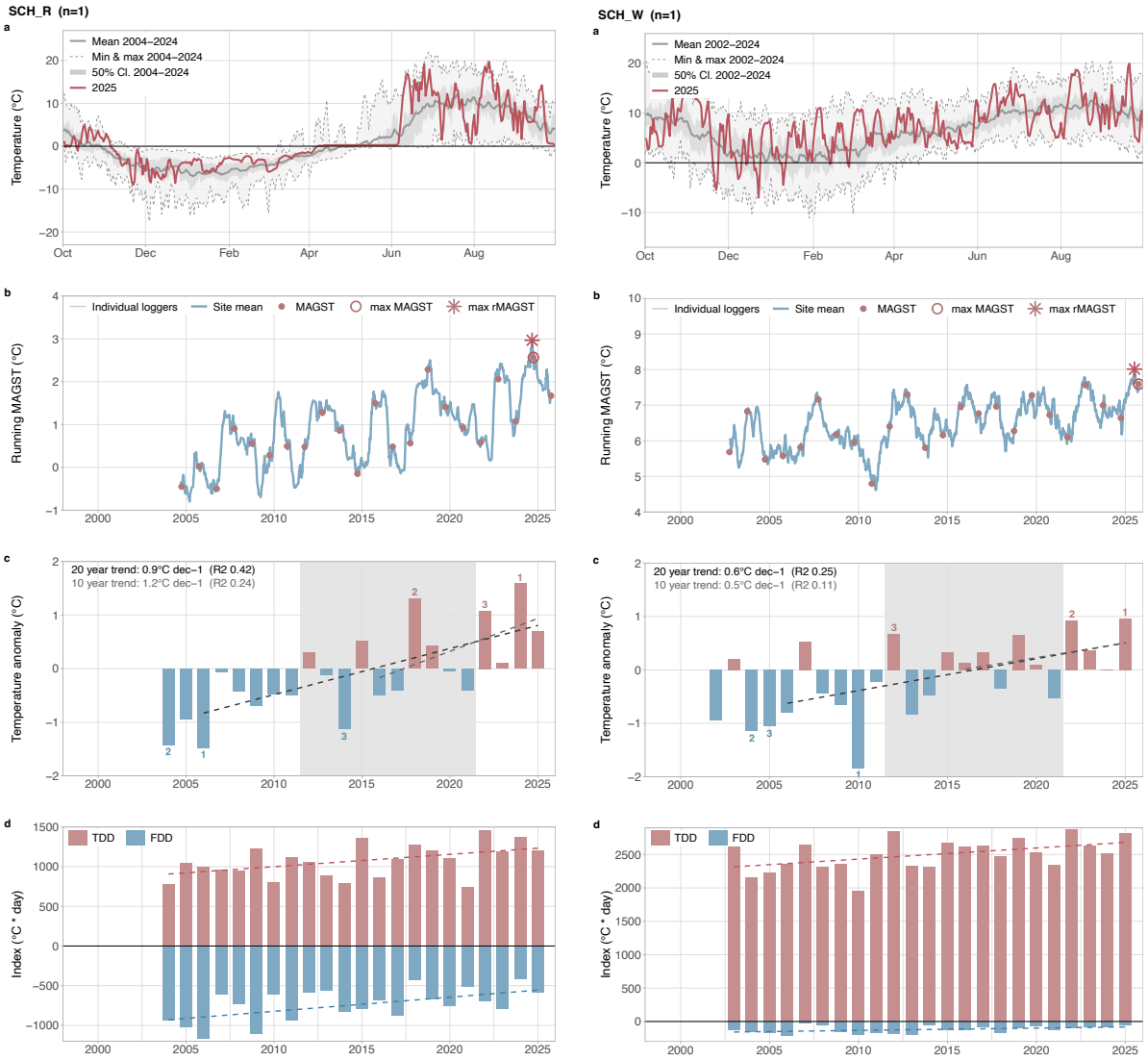

Figure 3.2. Ground surface temperatures at two bedrock sites at the Schilthorn with long and complete time series: bedrock with winter snow cover (SCH_R, left) and steep bedrock without a thicker winter snow cover (SCH_W, right). a) Daily mean GST at the sites during the hydrological year 2025 compared to all previous years. b) Running annual mean (rMAGST, thick blue line), mean annual ground surface temperature (MAGST) is shown with orange dots, the maximum MAGST of the time series with a circle, and the maximum rMAGST with an asterisk. c) Departure of the MAGST from the 2012–2021 decadal mean. Linear trends for the last one and two decades are shown with dashed lines. d) Ground thawing and freezing indexes with linear trend lines.

the MAGST exceeded the 2012–2021 decadal mean by 0.2–1 °C at 13 of 16 sites (81%), indicating generally warm conditions near the ground surface.

A new record MAGST was observed at the steep bedrock site SCH_W, where GST measurements have been conducted since 2002 (Figure 3.2). Here, MAGST in 2025 was 0.9 °C higher than in the previous year and nearly 1 °C above the decadal mean, which likely reflects the record SAT (see Chapter 2). In contrast, MAGST lower than the 2012–2021 decadal mean was recorded at three rock glacier sites in Ticino (SCE, Figure 3.1) and in the Engadine (COR and MUR). This is likely due to a late and thin snow cover in Eastern Switzerland in winter 2025.

The trailing running mean annual ground surface temperature (rMAGST, Figure 3.1b, Figure 3.2b, Figure 3.3) reveals more temporal variability than the MAGTS value. It generally decreased during the first half of the hydrological year 2025 until June 2025, increased during two months until end of July and decreased again until the end of the hydrological year. This clearly shows the influence of

the snow cover on thermal conditions at the ground surface. Even though SAT reached record values in 2025, this signal was only reflected at a steep bedrock site and not at the other sites, because they were snow-covered during late winter and spring. In addition, the ground surface could cool because the snow cover in winter 2025 formed very late (see Chapter 2). This situation is the opposite of the previous year, when an early snow cover insulated heat in the ground and led to very high MAGST values (PERMOS 2025).

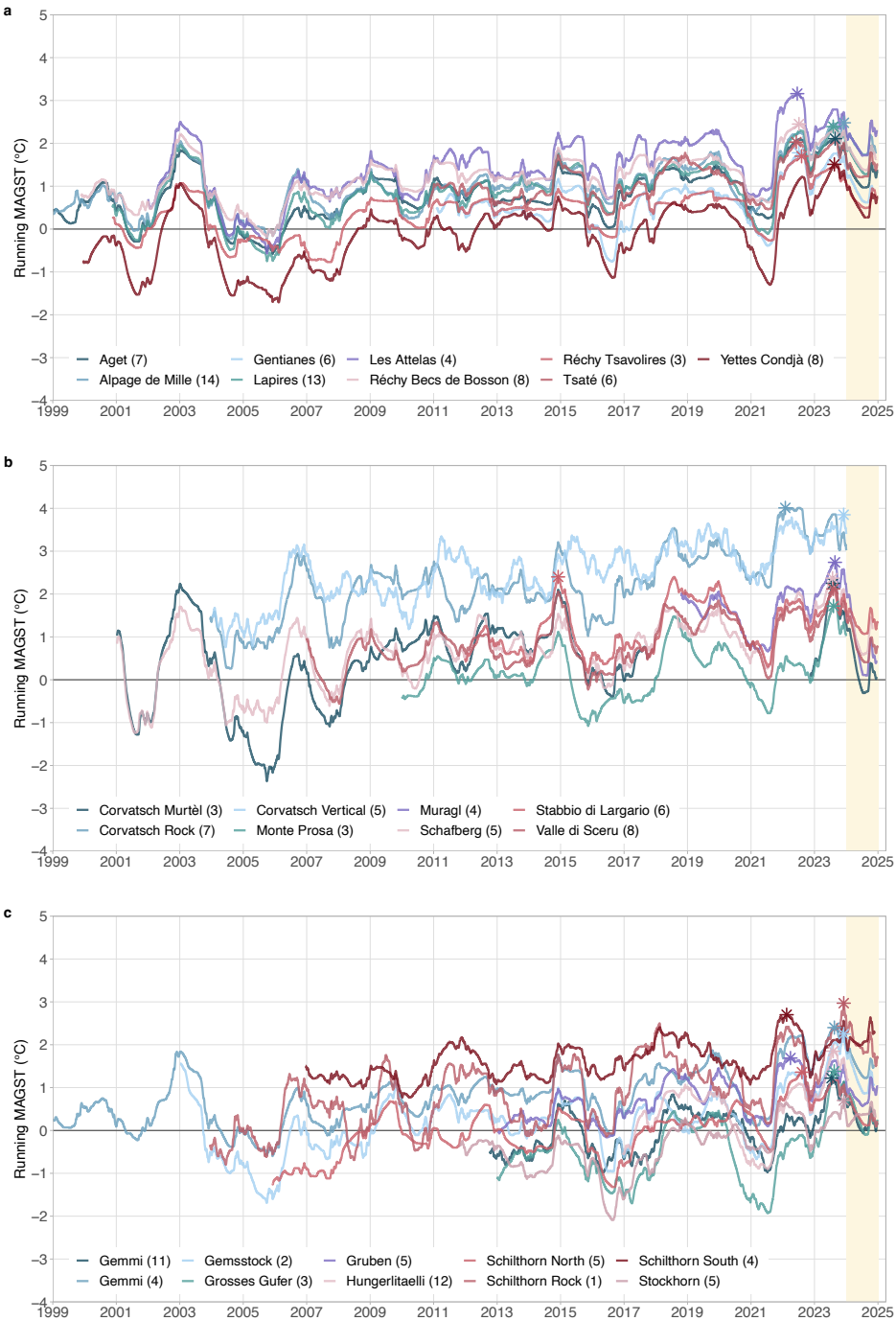

Figure 3.3. Trailing running mean annual ground surface temperature (rMAGST) for sites in (a) the Lower Valais, (b) the eastern and Southern Swiss Alps, and (c) the Upper Valais, central and Northern Swiss Alps. The maximum value of rMAGST is indicated with an asterisk. The reporting period is highlighted with a yellow background. Corvatsch Rock, Corvatsch Vertical and Gemsstock are measured in flat and near-vertical bedrock, all other sites are in unconsolidated material (rock glaciers and talus slopes). Series depict site averages of several individual time series (cf. number of loggers in brackets).

For the 16 report groups that cover 20 years or more, the GST have increased by 0.5–0.9 °C dec^{-1} during the 20-year period 2006–2025 (linear regression on MAGST). The highest warming rates are observed in steep bedrock snow-free sites, the lowest rates are observed in coarse blocky terrain.

The Ground Freezing Index (GFI) is defined as the sum of the negative daily temperatures during a hydrological year and is an indication of how cold a winter season was. The Ground Thawing Index (GTI) is defined as the annual sum of positive daily temperatures and is an indication of how warm the thawing season was. It can only be determined for sites with data extending to the end of the hydrological year. In general, both GFI (Figures 3.1d and 3.2d, blue bars) and GTI (Figures 3.1d and 3.2d, red bars) were higher in 2025 than in 2024. This points to the cold winter conditions and the warm summer conditions.

3.2 Active layer thickness

The ALT is calculated by linear interpolation of daily ground temperature time series measured at multiple depths in boreholes, using the lowermost sensor in the active layer (T>0 °C) and the uppermost sensor in the permafrost (T≤0 °C). Because freeze/thaw processes and varying ground characteristics in the uppermost meters result in a non-linear temperature profile, changes in ALT must be interpreted with care, particularly in ice-rich ground. The direction of the trends and the magnitude of the variations are nevertheless considered robust.

Table 3.1. Active layer thickness (ALT, in meters) in 2025 and corresponding date for PERMOS boreholes, as well as the difference to the previous year and the year with the maximum ALT recorded. Values in italics are intermediate values because the data does not cover the entire thawing period. Boreholes in which only an approximate range of the ALT can be determined (e.g., due to broken or unreliable sensors or data gaps) are also listed.

Borehole	ALT 2025	Date	Diff. 2024	First year	Max year	Comment
Attelas 0108	5.1	2025-09-19	0.1	2009	2025	Available data ends 2025-09-19
Attelas 0208	6.0	2025-09-05	<0.1	2009	2025	Available data ends 2025-09-19
Murtèl-Corvatsch 0315	4.8	2025-06-15	–0.1	2016	2024	New depths used for interpolation due to broken sensors.
Gentianes 0102	5.2	2025-09-05	–0.4	2003	2024	Available data ends 2025-09-15
Gentianes 0222	4.6	2025-09-10	0.5	2023	2025	
Lapires 0198	7.0	2025-09-10	0.3	1999	2025	
Lapires 1208	6.8	2025-10-06	–0.5	2010	2024	
Muot da Barba P. 0296	–	–	–	1997	–	ALT <4.6 m, no sensor left in ALT
Muot da Barba P. 0319	3.0	2025-09-28	–0.2	2020	2024	
Muragl 0424	4.9	2025-08-31	<0.1	2024	2024	
Ritigraben 0102	5.6	2024-08-23	<0.1	2002	2024	Thermistor at 4 m may be inconsistent
Schafberg 0190	–	–	–	2005	2024	ALT >4.2 m, available data ends 2025-07-31
Schafberg 0290	–	–	–	1997	2024	ALT >3.3 m, available data ends 2025-08-02
Schilthorn 5198	–	–	–	1998	2022	No ALT after 2022, no refreezing
Schilthorn 5200	–	–	–	2001	2017	No ALT after 2017, no refreezing, permafrost table in 2025 between 12 and 17 m
Schilthorn 5318	–	–	–	2019	2021	No ALT after 2021, no refreezing, permafrost table in 2025 at ca. 18 m
Stockhorn 6000	5.5	2025-10-07	–0.3	2001	2024	
Stockhorn 6100	6.7	2025-10-14	0.2	2001	2024	

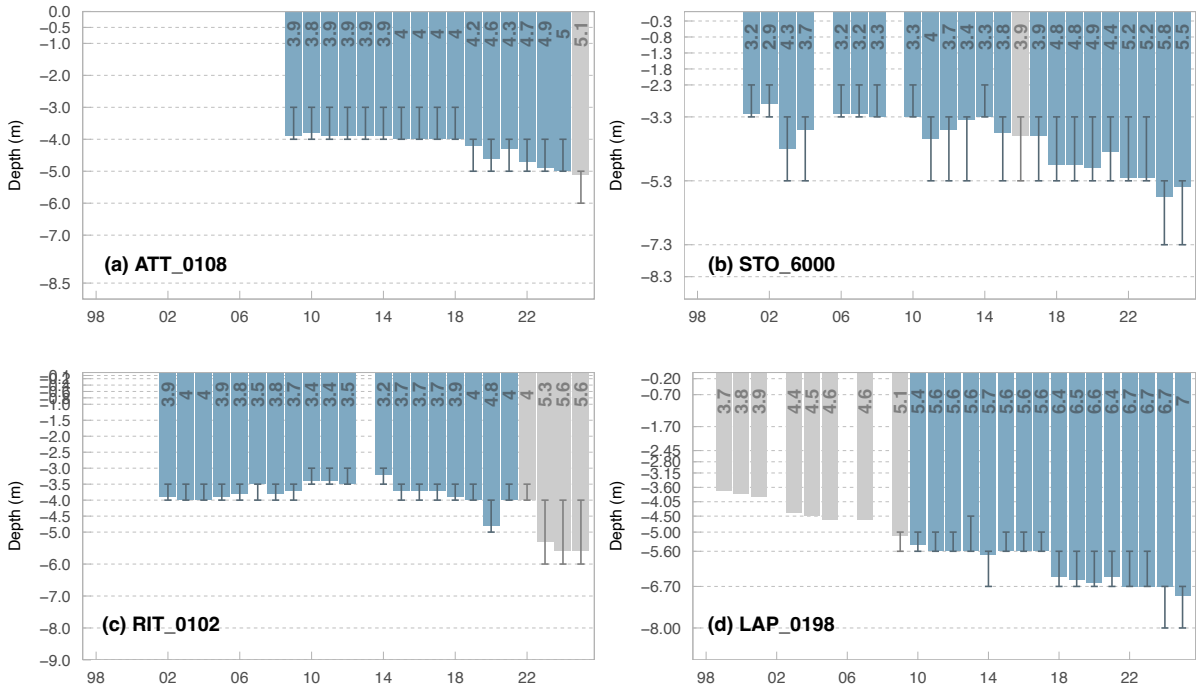

Figure 3.4. Active layer thickness (ALT) derived from ground temperature time series measured in the Attelas talus slope (a), on the Stockhorn plateau (b), in the Ritigrabe rock glacier (c), and in the Lapires talus slope (d). The uncertainty bars are defined by the thermistors used to interpolate the ALT (thermistor above and below 0 °C). Grey colours indicate estimated ALT due to questionable data quality (e.g. in case a sensor is not fully reliable) or when the available data does not fully cover the thawing period 2025.

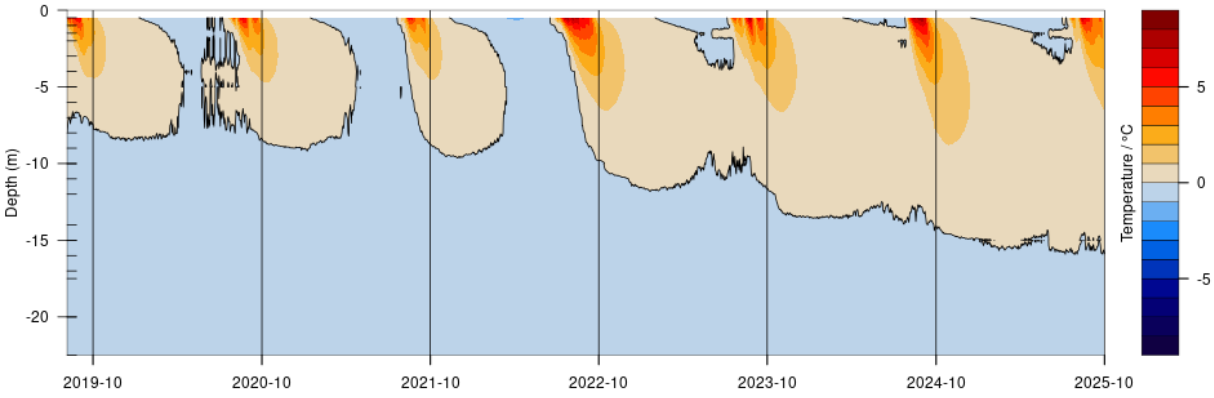

Figure 3.5. Permafrost temperature evolution at the Schilthorn in the Bernses Alps in borehole SCH_5318 drilled in 2018. The active layer did not refreeze in winter after 2022 and a supra-permafrost talik formed. The permafrost table is slowly deepening, the thermistor at 16 m depth is at about 0 °C at the end of the hydrological year 2025 and at 17 m depth temperatures are still below 0 °C.

The ALT for the year 2025 could be determined for 12 of 24 boreholes at 9 sites (Table 3.1, Figure 3.4). For 3 of these boreholes the calculated ALT is a first estimate because the available data do not yet cover the end of the thawing period and the ALT may be larger (ATT_0108, ATT_0208, GEN_0102). For four boreholes, only approximate range of ALT can be given due data ending at the end of July (SBE_0190 and SBE_0290) or due to defective sensors in the ALT (MBP_0296).

On Schilthorn, a supra-permafrost talik formed in recent years and no ALT can be determined due to the absence of refreezing of the thaw layer. For the three boreholes on Schilthorn, the thickness of the unfrozen layer above the remaining permafrost is in the order of 17 m in 2025 (Figure 3.5).

In the other boreholes, the calculation of ALT is not or no longer possible. Reasons are no permafrost (MUR_0199, GEM_0106) or no or erroneous sensors at the relevant depths (JFR_0195, MUR_0499, LAP_1108, TSA_117). ALT values in 2025 were between 3.0 m (MBP_0319) and 7.0 m (LAP_0198) and were similar as in the previous year with some values larger and some lower (Table 3.1, Figure 3.4), partly even in different borehole at the same site.

3.3 Permafrost temperatures

Continuous permafrost temperatures are measured at multiple depths in 24 boreholes at 14 sites in 2025 (Table 1.1). All boreholes are equipped with multi-sensor cables and automatic logging systems. Many sites transmit data automatically, while at other data is collected on site once a year. For the latter, records often do not yet cover the complete hydrological year up to October 2025 as field work typically takes place earlier. Recording interval range from 1 to 24 h, depending on the instrumentation. Observations follow established guidelines for long-term borehole temperature measurements (Noetzli et al. 2021; Streletskiy et al. 2022; Irrgang et al. 2024).

Permafrost temperature data are quality-checked for outliers and erroneous sensors, and additional inconsistencies – such as noise, sudden temperature jumps or sensor drift – are identified through visual inspection and plausibility checks (i.e., consistency with neighbouring data). The time series are then aggregated to daily, monthly, and annual means using depth-dependent data completeness criteria (cf. also Noetzli et al. 2024). Challenges related to the long-term operation of the borehole stations were described in the last report (PERMOS 2025).

During the hydrological year 2025, the mean annual permafrost temperatures (MAPT) at 10 m depth was lower compared to 2024 in 3 out of 24 boreholes with data available for 2025, equal (difference <0.1 °C) in 7 boreholes and slightly higher by 0.1–0.2 °C in 10 boreholes. For 17 boreholes at 11 sites, the 2025 MAPT at 10 m depth was a record when compared to the entire time series. MAPT thus continued the long-term warming trend of the past two decades. No clear pattern of these most recent short-term changes can be discerned regarding ground ice content or landform.

At 20 m depth, temperatures react with more delay to changes in GST and changes from one year to the next are smaller. Here, the permafrost temperatures increased by 0.1–0.2 °C in 2025 compared to the previous year in 6 out of 19 boreholes. At 13 boreholes at 9 sites, the MAPT at 20 m depth in 2025 is a record level compared to the entire time series.

On a decadal perspective, observed permafrost temperatures in the Swiss Alps have increased up to 1.1 °C at 10 m depth in the decade 2015–2024, with a mean of 0.4 °C (see Noetzli et al. 2025). The highest change rates at the PERMOS sites are obtained for the bedrock site on Jungfrau East Ridge with a warming of 1.1 °C for 2016–2025. A slight cooling was observed at the Ritigraben rock glacier as well as on the South side of Gemsstock in this period, with –0.1 °C. A lower mean change rate of 0.2 °C dec^{-1} was observed at 20 m depth (ranging from –0.1 to 0.5 °C dec^{-1}), which results from the increasing delay in the temperature signal penetrating to larger depth. At 20 m depth, the strongest warming for 2016–2025 was observed at Stockhorn with 0.6 °C (0.9 °C at 10 m depth at this site, at Jungfraujoch no measurements are available at 20 m depth).

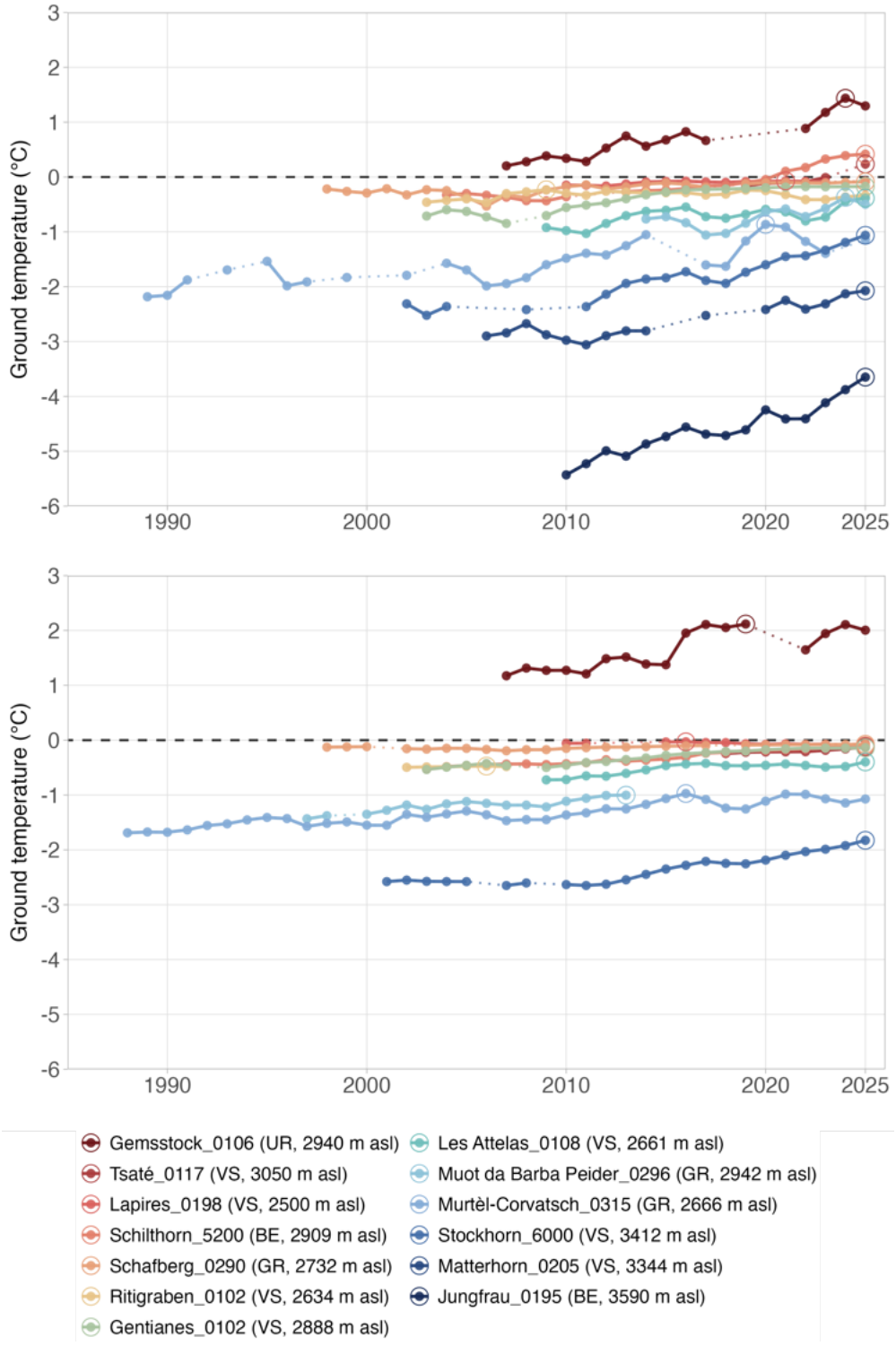

Figure 3.6. Ground temperatures measured in selected PERMOS boreholes at 10 m (top) and 20 m depth (bottom). The temperatures are shown as mean values for hydrological years. Maximum values for each time series are shown with circles.

To detect changes in warm or near 0 °C permafrost, additional measurements sensitive to changes in ground ice and liquid water content are needed to observe changes in the permafrost until the frozen material has thawed entirely (see Section 4).

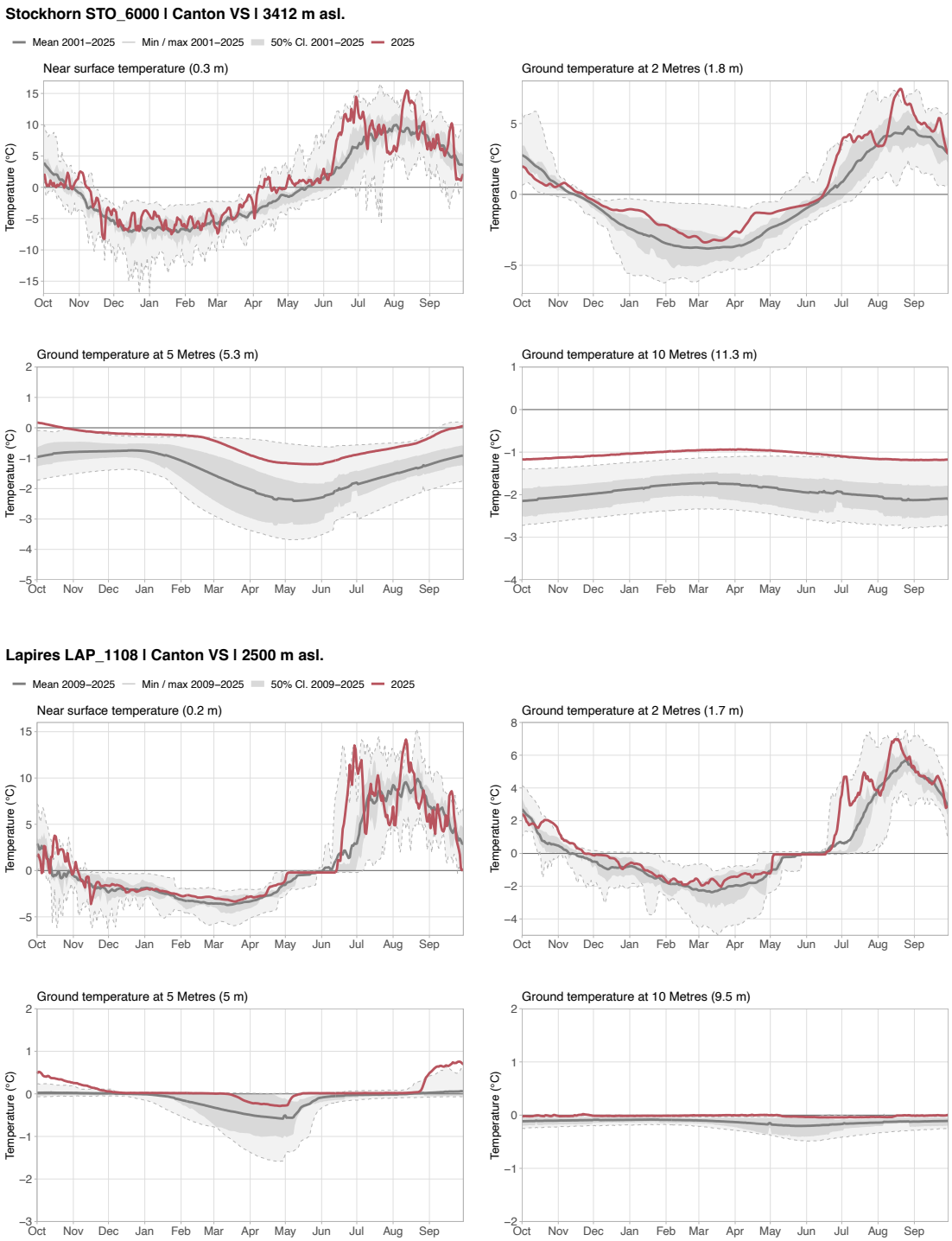

Figure 3.7. Evolution of daily ground temperatures during the hydrological year 2025 at different depths in the uppermost 10 m of the borehole on Stockhorn above Zermatt at 3400 m asl. (STO_6000, above) and in the Lapires talus slope at 2600 m asl (LAP_1108, below). The ground temperatures measured in the hydrological year 2025 are

4 Electrical resistivities of permafrost

4.1 Background

Electrical Resistivity Tomography (ERT) exploits the different electrical properties of the subsurface components. This method is sensitive to the presence of liquid water in the substrate and well suited to distinguish frozen from unfrozen terrain. By repeating ERT surveys with identical measurement setup (profile location and geometry), changes in subsurface properties and changes in liquid water and ice content in the ground can be assessed, which cannot be detected with the thermal measurements described above, as ice and water can coexist at near 0 °C temperatures. In a permafrost environment, decreasing electrical resistivities indicate an increase of the ratio between liquid water and ice content, pointing to an overall ground ice melt and/or increase in liquid water content. Conversely, increasing electrical resistivities can be caused by an increase of the ground ice content and/or a decrease in liquid water content, but may also indicate an overall drying, e. g. in the active layer.

4.2 Conditions in 2025

Electrical resistivities are measured at five PERMOS sites along profiles of 96 to 235 m length, along which 43–50 electrodes are permanently installed (stainless steel rods) and connected by cables to a central box, to which the measurement device can be connected (see Figure 4.1). Measurements are performed annually at the end of summer (end of August to October). Measured resistivities are quality controlled and inverted following the procedure described in Mollaret et al. (2019).

Amongst the five ERT monitoring sites, three were visited in 2025. The measurements at Les Attelas have been discontinued since 2023 due to safety issues caused by rockfall activity. At Murtèl-Corvatsch, the profile is awaiting repairs following damages caused by rockfall in 2023. Repairs are planned in early summer 2026 and monitoring will resume at the site.

Figure 4.1. Electrical Resistivity Tomography (ERT) monitoring installation at Stockhorn. Photo: C. Hilbich.

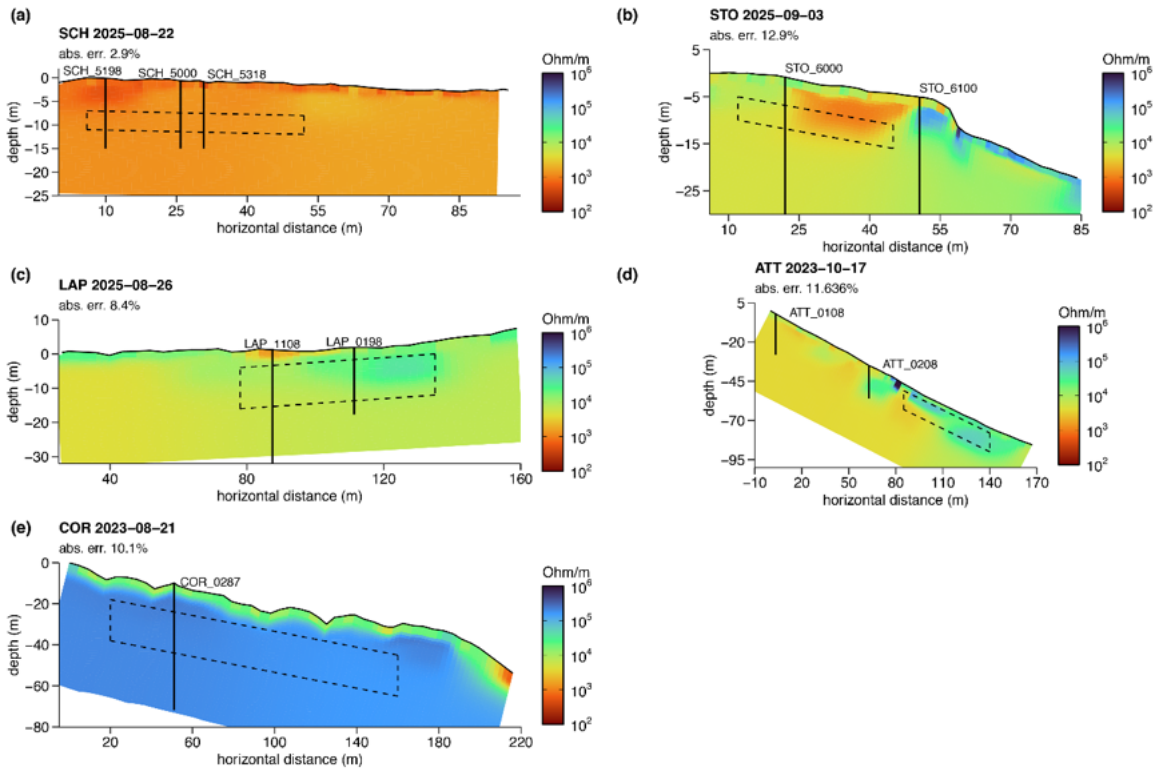

Figure 4.2. Electrical Resistivity Tomograms showing the resistivity distribution at two bedrock sites (Schilthorn, a and Stockhorn, b), two talus slopes (Lapires, c and Les Attelas, d) and one rock glacier (Murtèl-Corvatsch e) in 2025 (a–c) and 2023 (d–e). The representative zones used to derive the time series in Figure 4.3 are indicated with dashed boxes and the borehole locations are shown with vertical black lines.

The electrical resistivities measured at the five PERMOS sites span several orders of magnitude due to the site specific different sub-surface characteristics (i.e. ice-content, sub-surface type, Figure 4.2). The lowest values are obtained at Schilthorn (~1'500 Ωm), an ice-poor bedrock site with permafrost temperatures close to 0 °C. The highest resistivities are measured at Murtèl-Corvatsch (~200'000 Ωm), a rock glacier site characterized by a coarse blocky surface and an ice rich core.

Spatially averaged resistivity values are computed for manually selected zones within the ERT tomograms to perform inter-site comparison and analyse the temporal evolution (Figure 4.2). These zones encompass the largest possible homogeneous part of the permafrost (based on temperature and resistivity) and the part of the tomogram with the highest measurement sensitivity and quality (i.e. excluding the lateral and deep edges of the tomogram). The active layer is excluded wherever possible to focus on the permafrost. The representative zone at Schilthorn is no longer in permafrost since 2024 (see Figure 3.5).

Since the start of the observations, resistivities measured in the permafrost generally decreased at all sites (Figure 4.3). This trend is consistent with the increasing ALT and permafrost temperatures and indicates a general increase in liquid water content in the permafrost, which is considered a direct consequence of ground ice melt and enhanced infiltration of water.

The quality of the ERT surveys in 2025 was satisfactory (70–98% of data remaining after filtering and 2.8–9.5% absolute error of the final inversion, see Mollaret et al. 2019). At Stockhorn, resistivities within the representative zone increased by 26% compared to 2024 and by 7% compared to 2023. At Lapires the resistivity decreased by 3% compared to 2024 and at Schilthorn by 1%.

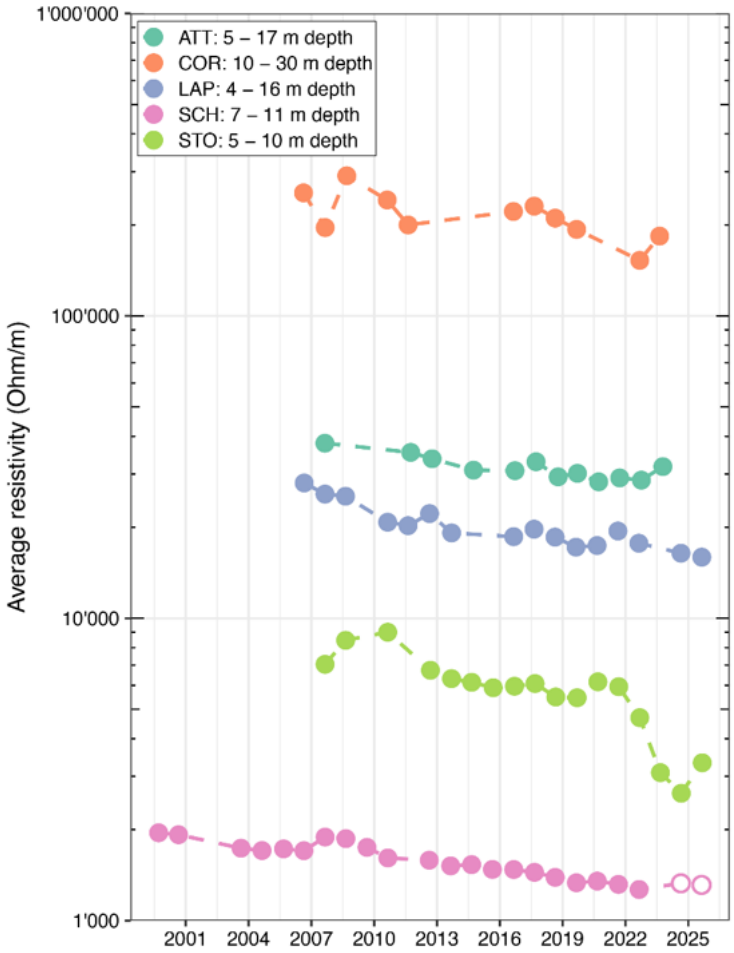

Figure 4.3. Average electrical resistivities of the representative zones (see Figure 4.2) at the end of summer for the 5 ERT sites in the PERMOS Network. Note that at Schilthorn the representative zone is no longer in permafrost condition since 2024 due to the formation of a talik (indicated by an empty symbol).

Stockhorn is a bedrock site with comparatively low ice content, where ground temperatures are mostly controlled by conductive heat transport. The large resistivity increase is in line with the recorded ALT decrease in 2025 (STO_6000, see Table 3.1) due to the winter cooling. Lapires is a coarse blocky site with higher ground ice content, where conductive heat transport occurs in addition to latent heat exchange and heat convection/advection via ventilation within the coarse blocky material. The small resistivity change (–3%) observed in 2025 is in line with the increase in ALT and permafrost temperature in 2025 at borehole LAP_0198, which is located on the ERT profile. At Schilthorn ground ice is no longer present within the representative zone and the temperatures remained above 0 °C throughout the year since 2024 (see Figure 3.5). The small resistivity variation observed in 2025 (–1%) could indicate that the thawed layer above the permafrost remained in similar conditions as in 2024 (ice free and with similar liquid water content).

5 Rock glacier velocity

5.1 Background

The kinematics of creeping permafrost landforms such as rock glaciers are primarily controlled by their intrinsic characteristics (e.g., internal structure and composition, topographical and geological settings), whereas changes over time are driven by weather conditions, water availability and climate processes. Inter-annual changes in rock glacier velocity (RGV) at the surface reflect the deformation changes at the shear horizon (Cicoira et al. 2021), which is typically located at 15–20 m depth in the permafrost body. The velocity changes are related to the evolution of permafrost temperature and liquid water content between the permafrost table and the shear horizon. At inter-annual time scale, RGV follows an exponential relation with multi-annual GST forcing (i.e., increasing GST lead to an increase in velocity and conversely, see Staub et al. 2016). Inter-annual RGV changes further depend on the snow cover thickness, which affects both ground temperature and water availability.

RGV also exhibits seasonal variations related to those of snow cover and ground temperature. Whereas their amplitude is diverse, ranging from a ratio of 1/1.1 to 1/10, the seasonal kinematics follows a repetitive pattern with minimal velocities at start of the snowmelt season (around May), a strong acceleration during snowmelt and maxima in fall-early winter (October-November).

Surface velocities of rock glaciers are determined by annual terrestrial geodetic surveys (TGS, Section 5.1) performed at the end of summer (August–October) as well as with permanently installed GNSS devices (Section 5.2). The two complementary methods allow to capture the seasonal velocity variations (permanent GNSS) and their spatially distributed inter-annual changes (TGS) (see also Saibene et al. 2026).

Figure 5.1. Permanent GNSS device on the Stabbio di Largario rock glacier (Ticino Alps). Photo: C. Scapozza.

5.1 Annual rock glacier velocity

Annual TGS are performed with high precision differential GNSS or total stations. The positions of selected boulders (10–100 points per site covering the entire landform and stable areas nearby) are measured annually and surface velocities derived. Control points (i.e., points located on stable areas) are used to calibrate and adjust the measured positions with an average accuracy in the range of mm

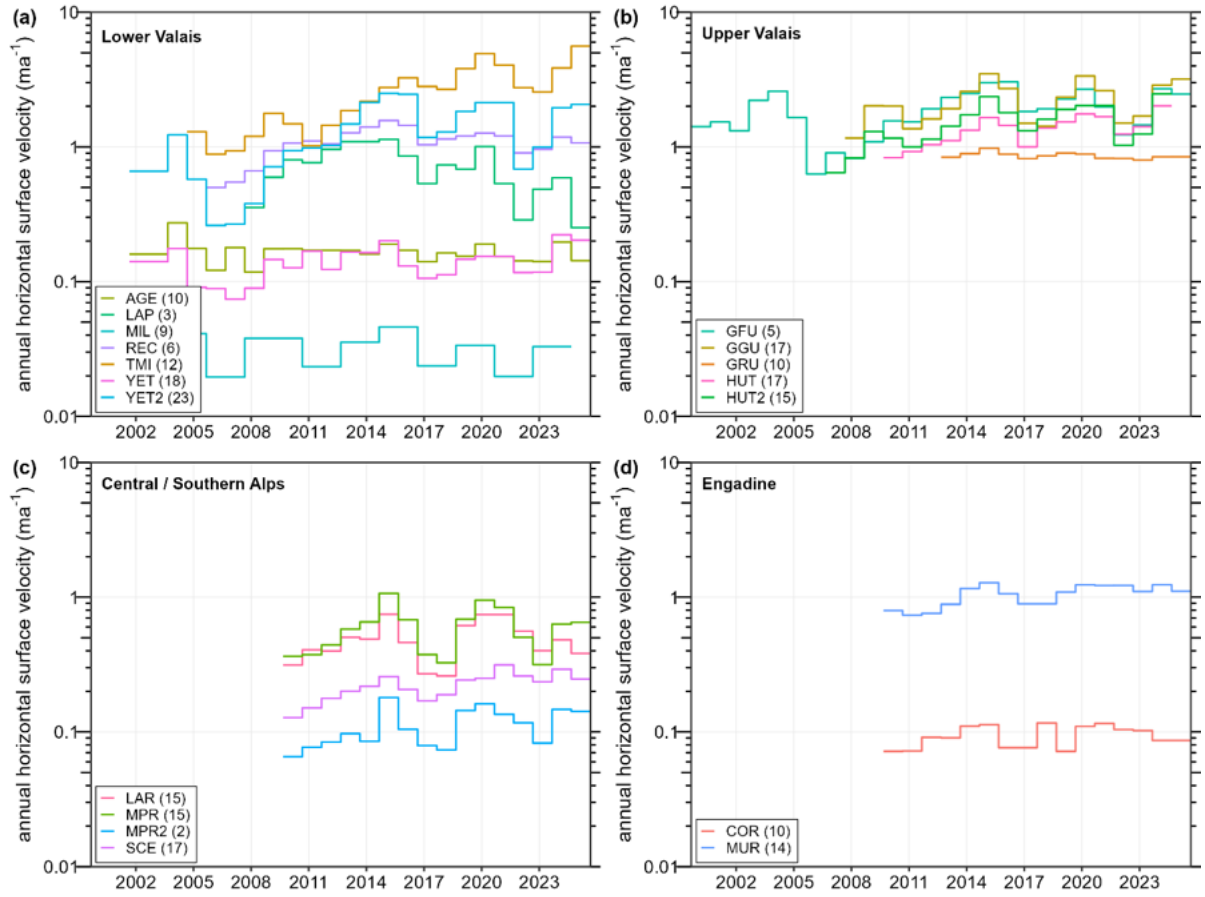

Figure 5.2. Pattern of horizontal surface velocities of 18 rock glacier lobes in the Swiss Alps, divided into four topo-climatic regions. The number of reference points for each site is indicated in brackets next to the site abbreviations (full site names can be found in Table 1.1).

to cm. For each rock glacier, a set of reference points is defined based on their spatial distribution (i.e., located within the area of the rock glacier where surface displacements are dominantly related to permafrost creep), data quality and completeness. The reference points are used to compute site averages (Figures 5.2 and 5.3, see also Kellerer-Pirklbauer et al. 2026).

In 2025, TGS measurements were performed at 16 of 18 rock glaciers of the network. Measurements in Hungerlitaelli (HUT1 and HUT2) were not possible due to early snow fall in autumn. RGV in 2025 generally decreased at all sites but 4, where RGV slightly increased (Figure 5.2). Compared to 2024, an average decrease of –13% was observed in the Swiss Alps. Regional decreases range from –5% in the Lower Valais to –22% in the Engadine. The maximum decrease in 2025 was observed at Sceru in Ticino (SCE, –22%), whereas the maximum increase in 2025 was observed at Grosses Gufer in the Upper Valais (GGU, +14%). Velocity changes in 2025 are consistent with the lower GST, which reflect the important winter cooling in 2024/25 compared to 2023/24 (see Sections 2 and 3).

Despite regional differences and variable landform size, morphology, and velocity range, a coherent evolution of rock glacier velocity can be identified in the Swiss Alps (Figure 5.3a). Since 2000, velocities have generally increased with marked inter-annual variability. Periods of velocity decrease include 2004–2006, 2016–2018 and 2021–2022 (Bast et al. 2024). Rates of velocity increase are highest since 2010, and maximum velocities were recorded in 2015 and/or 2020 depending on the

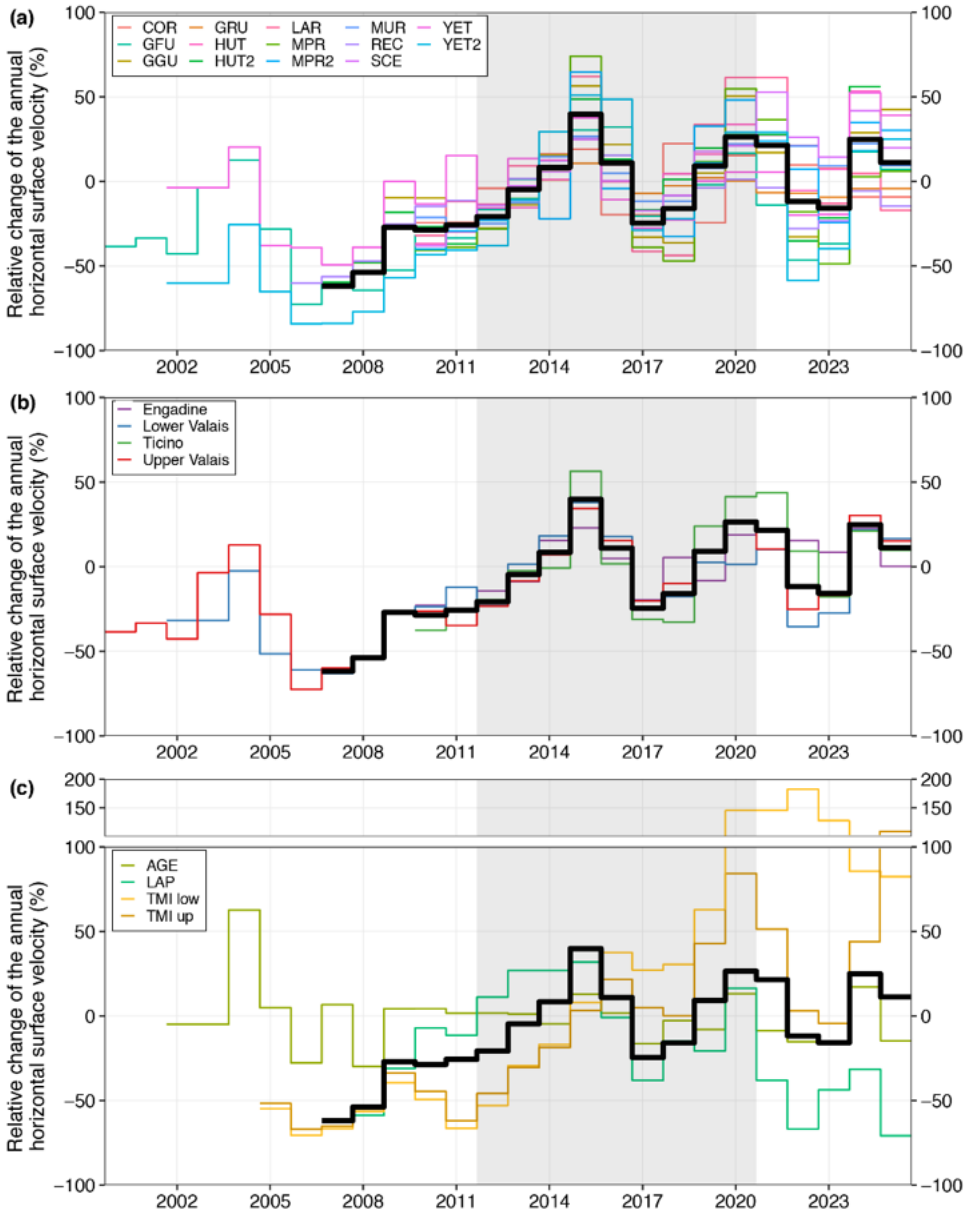

Figure 5.3. Mean annual horizontal surface velocity derived from terrestrial geodetic surveys relative to the reference period 2011–2020 (grey area). The black line is the average of all sites (excluding Tsarmine (TMI), Aget (AGE) and Lapires (LAP)). (a) 14 monitored rock glacier lobes (for site abbreviations see Table 1.1). (b) Average for the four topo-climatic regions of the Swiss Alps. (c) Three atypical rock glaciers (note that TMI is divided into two separate areas).

site. Similar rock glacier velocity patterns were also reported for the French, Italian and Austrian Alps (Kellerer-Pirklbauer et al. 2024)

Three of the rock glaciers in the PERMOS Network do not follow this general pattern (Figure 5.3c). Since 2015, rock glacier Tsarmine (TMI) has been accelerating more strongly, especially in its lowermost part, while rock glaciers Aget (AGE) and Lapires (LAP) have been decelerating. At Aget the velocity decrease was observed from the start of the measurements in 2001 until around 2013, whereas at Lapires the consistent deceleration started in 2015 and is still ongoing. These contrasting kinematics are also interpreted as a response to climate warming: a deceleration typically results from in-situ permafrost degradation (i.e., thinning of the permafrost body above the shear horizon and/or increased friction at the shear horizon, e.g., due to freezing as a result of a snow-poor winter), whereas an exceptional acceleration points to an ongoing destabilization (see Roer et al. 2008). In both cases, these mechanisms overprint the general rock glacier evolution related to climate effects.

In 2025, the upper part of Tsarmine rock glacier showed a 65% increase in velocity, which contrasts with the overall RGV observation in the Swiss Alps. While this part was moving faster than any of the observed rock glaciers (~3–5 m a^{-1}), its inter-annual variation followed the average behaviour up until 2025. This divergence could indicate the onset of destabilization of the upper part of Tsarmine rock glacier. At Aget and Lapires, similar interannual variations to the Swiss average are also observed although the overall trend at these sites is significantly different.

5.2 Seasonal rock glacier velocity

Permanent GNSS devices are installed on 8 rock glaciers of the PERMOS Network for continuous position measurements. The high temporal resolution of the data enables the computation of monthly to daily displacements (depending on the absolute velocity of the rock glacier). The raw data are post-processed using a double-difference processing scheme to obtain robust quality controlled daily positions. Small velocity variations (< ±0.1–0.2 m a^{-1}) can be influenced by different factors (e.g. snow pressure on the GNSS mast in winter, stability of the boulder in the terrain) and are potentially not representative of the general rock glacier motion (e.g. Wirz et al. 2014). To exclude such short-term variations and enhance the reliability of the data positions are filtered and aggregated with a 30-day moving window.

Figure 5.4 shows the seasonal evolution of surface velocities for two rock glaciers: Gemmi (GFU, Upper Valais), Grosses Gufer (GGU, Upper Valais). A typical seasonal pattern can be observed at all sites: i) decreasing velocities in winter with minima in April followed by ii) a strong acceleration at the beginning of summer (during snow melt) and iii) peak velocities observed at the end of summer (when GST are highest).

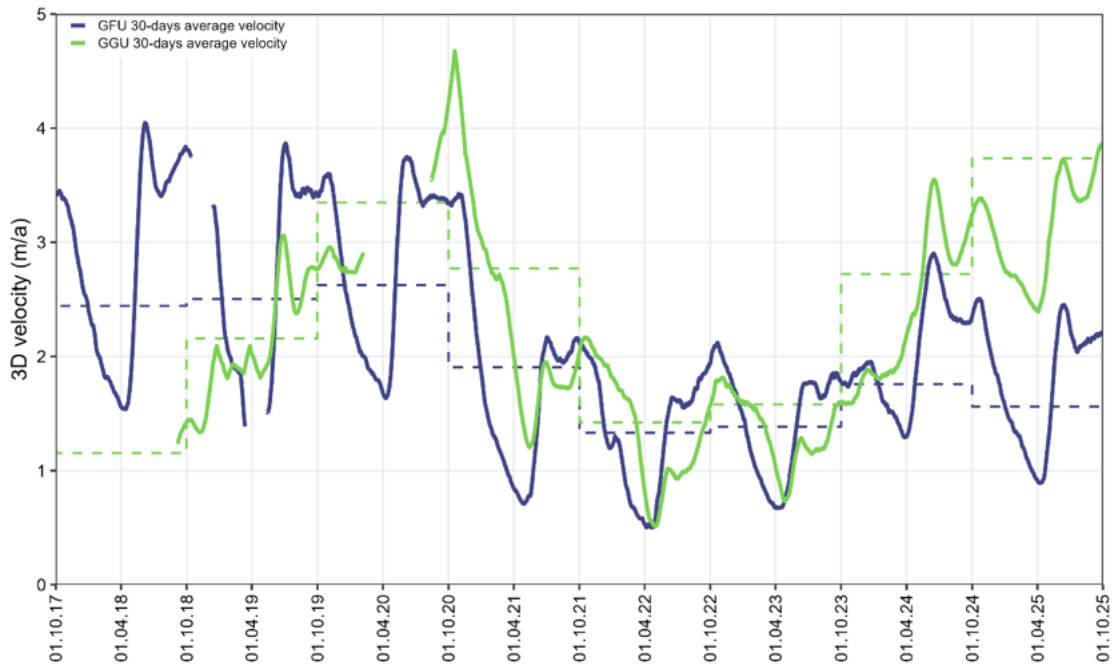

Figure 5.4. Evolution of the seasonal 3D surface velocity at the rock glaciers Gemmi (purple) and Grosses Gufer (green). The velocities are computed over 30-day periods. The dotted lines represent the annual surface velocity measured by TGS at the boulder closest to the GNSS device.

During the hydrological year 2025 rock glacier velocities followed the typical seasonal pattern. The winter deceleration was much more pronounced than in previous years, in line with the ground cooling observed near the surface during the snow-poor winter (Chapter 3.1). The acceleration following the snow melt period was in a similar range as in 2024 at Gemmi and Grosses Gufer, reaching marked velocity peaks at the beginning of the summer. At both sites the end of summer

peak has not yet been reached on 1 October 2025, although velocities at Grosses Gufer exceeded the values observed during the peak at the beginning of the summer. At the end of the hydrological year 2025, the velocity at Grosses Gufer was clearly higher than at the beginning of October 2024, whereas at Gemmi it was lower. This is confirmed by the annual average velocity observed using the terrestrial geodetical surveys (dashed lines in Figure 5.4). The main difference between the two sites, is the amplitude of the winter deceleration, which was more important at Gemmi (–72%) than at Grosses Gufer (–55%).

6 Rock slope failures in permafrost

Permafrost warming and degradation are expected to reduce slope stability and increase the probability of rock fall events in high mountain areas. The stability of permanently frozen rock faces (i.e. the general predisposition) depends on multiple factors including the geological structure (lithology, structure, fracturing) and the topography (e.g. Krautblatter et al. 2013; Gruber, and Haeberli 2007; Jacquemart et al. 2024) Permafrost changes affect shorter-term susceptibility of a rock slope to failure (i.e. the variable pre¬dispo¬sition, Fehlmann et al. 2016). Permafrost warming generally reduces the strength of the rock and ice-filled fractures (Mellor 1973; Davies et al. 2001; Mamot et al. 2021). Ice melt in rock fractures can promote deep water infiltration, leading to rapid temperature changes and increased hydrostatic pressure (Hasler et al. 2011; Offer et al. 2025).

To assess when and under which geological, thermal or topographical conditions rock slope failures occur in permafrost areas, a dedicated data base is maintained by the WSL Institute for Snow and Avalanche Research SLF within PERMOS. This documentation supports scientific analyses and builds on earlier compilations (Noetzli et al. 2003; Fischer et al. 2012), which have continuously been updated and complemented in the past decades. The data are verified using satellite imagery, drone surveys, terrestrial photographs and reports. Inclusion criteria are i) the starting zone is in the permafrost area and ii) the volume exceeds 1000 m^3. Primary data sources include media reports and observations from mountain professionals and users (e.g., guides, hut wardens, mountaineers, researchers, and hazard managers). Because no operational Swiss rock fall observer network exists, the dataset is subject to a significant observervational bias. Large events are well documented, whereas smaller failures are likely not consistently recorded. Reporting frequency and data completemenss likely increase in recent years due to expanded recreational mountain activities, access to mobile devices and growing awareness of the topic.

The most complete events from this data set are accessible via the PERMOS Data Portal. In the calendar year 2025, eight events from permafrost slopes were added with estimated volumes between 1000 to 6 Mio m^3. All events had their starting zone in north-facing slopes in permafrost areas and occurred between May and October (Figure 6.1).

In May 2025 a series of large rock slope failures occurred in the snow-covered NE facing permafrost

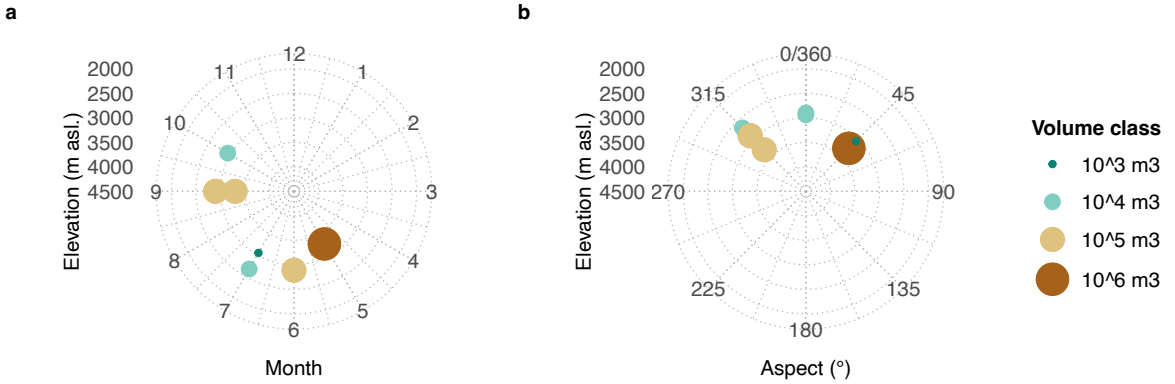

Figure 6.1. Rock slope failures from permafrost slopes during the calendar year 2025 plotted by volume class and elevation vs month (a) and slope aspect (b).

rock slopes on the Kleines Nesthorn above Blatten (Lötschental, Canton Valais). A total of around 6 million cubic metres of rock landed on the underlying glacier, the Birchgletscher, which failed spectacularly on May 28. The huge rock-ice avalanche buried large parts of the previously evacuated village of Blatten and killed one person. The processes leading to this particularly destructive chain of events are currently being investigated by an interdisciplinary group of researchers.

Figure 6.2. Rock fall deposit at Bocktschingel (UR) on the 14 June 2025 with an estimated volume of 250'000 m³. Photo: L. Eggimann.

In mid-June a rock slope failure with a volume of around 250'000 m³ occurred in the North facing slope of Clariden-Boggtschingel (Canton Uri). The deposit flowed towards the Griess lake, narrowly missing it (Figure 6.2). Several smaller events occurred during the summer. In September several rock slope failures of considerable size were observed: following intense rainfall, a failure of 100'000 m³ occurred in the North face of the St. Annagrat above Andermatt (Canton Uri) on September 7, flowing around 800 m over and covering large parts of the St. Annagletscher with rock debris. A week later, approximately 500'000 m³ of rock failed in the uppermost North facing rock wall of Val Zuort (Canton Grisons), and the deposit flowed around 1 km over the underlying Vadret da Zuort glacier. At the end of September a rock slope failure was observed on Piz Tremoggia (Canton Grisons), which also landed on a glacier.

Note: The volumes of the documented events must be considered with care. The volume of the Kleines Nesthorn Bergsturz in Blatten was measured shortly after the event. The volumes of the other 2025 events were estimated, but cannot yet be corrected or confirmed, as aerial images are not yet available.

7 Conclusions

The Swiss Permafrost Monitoring Network PERMOS documents the state and changes of permafrost in the Swiss Alps based on field measurements of ground temperatures, electrical resistivities and rock glacier velocities. All observations show a consistent pattern of continued warming and permafrost degradation in the Swiss Alps since the start of PERMOS in 2000. The general trend is overlaid by inter-annual variations in response to annual meteorological conditions, particularly the timing and depth of the snow cover and air temperatures.

In summary, the hydrological year 2025 was characterized by a mild and very snow-poor winter, a mild spring, and very warm atmospheric conditions during summer and autumn. It was the warmest hydrological year in Switzerland above 1000 m asl since measurements began in 1864. These climate conditions led to the following conditions in the permafrost in the Swiss Alps (Figure 7.1):

- Ground surface temperatures were slightly lower than in the previous year but clearly above the decadal mean 2012–2021. The late and thin snow cover in winter 2025 led to a cooling at the ground surface despite warm atmospheric conditions. In very steep terrain where no snow cover can form, GST were higher than measured before.
- The lower GST compared to the previous year also led to smaller active layer thickness in 2025.
- Permafrost temperatures at 10 m depth were equal or slightly higher (0.1–0.2°C increase) than in 2024 for the majority of PERMOS boreholes. 17 of the 24 boreholes registered record high permafrost temperatures in 2025. At 20 m depth, permafrost temperatures remained at high level and 13 of the 14 boreholes registered new record in 2025.
- Permafrost electrical resistivities showed contrasting evolution in 2025, with a slight decrease at both the Lapires talus slope (–3%) and the Schilthorn bedrock site (–1%) and an increase at the high elevation bedrock site Stockhorn (+26%) compared to 2024. This reflects the different levels of ground surface cooling.
- Rock glacier velocity decreased at most of the surveyed sites. Compared to 2024, an average decrease of –13% was observed over the Swiss Alps with regional changes ranging from –5% in the Lower Valais to –22% in the Engadine. Seasonal observations show that this behaviour is mainly due to the marked winter deceleration due to ground surface cooling and efficient freezing of water in the rock glaciers.
- The most striking rock fall event in 2025 were the series of large rock slope failures from the snow-covered NE facing permafrost rock slopes on the Kleines Nesthorn above Blatten end of May 2025.

Overall, the permafrost observations during the hydrological year 2025 point to close to record warm permafrost conditions, offset only by winter cooling at the ground surface due to the snow-poor winter. Active layer thickness, permafrost resistivity and rock glacier velocity show contrasting signals due to the different magnitude of ground surface cooling at the different sites.

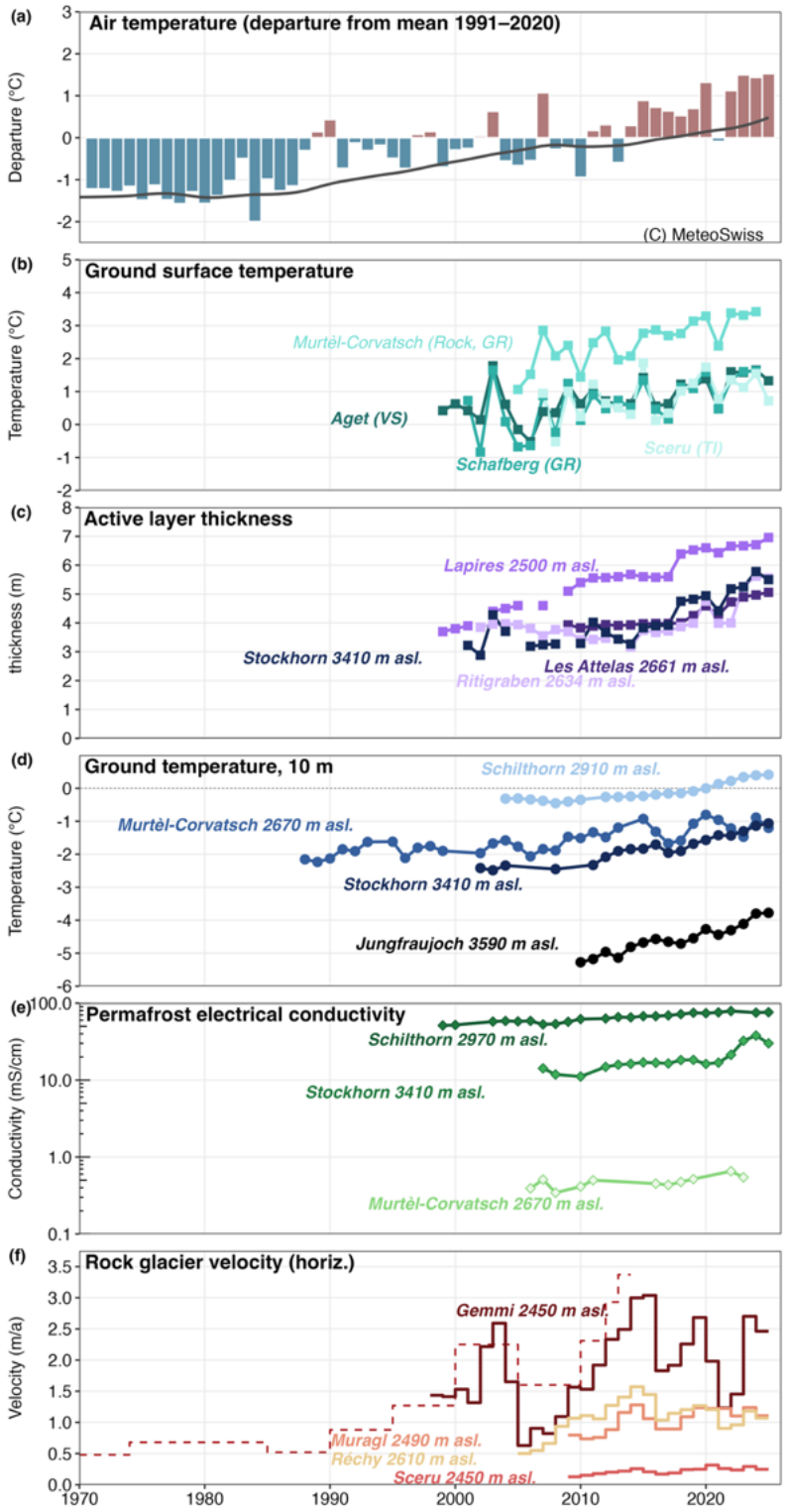

Figure 7.1. Evolution of the key observation elements of the Swiss permafrost monitoring: a) anomaly of annual air temperatures to the 1991–2020 climate norm period and 20year running mean (data source: MeteoSwiss, homogenized data series for Swiss stations above 1000 m asl), b) mean annual ground surface temperature, c) active layer thickness, d) annual mean permafrost temperatures at 10 m depth, e) permafrost electrical conductivity, and f) rock glacier velocity. The dashed red line in (f) represents the horizontal surface velocity for rock glacier Gemmi obtained by aerial photogrammetry. All annual mean values relate to hydrological years (October–September).

Acknowledgements

The site installation and maintenance, fieldwork and data preprocessing were performed by the seven partner institutions of the Swiss Permafrost Monitoring Network PERMOS: The Swiss Federal Institute of Technology (ETH Zurich) through their Laboratories of Hydraulics, Hydrology and Glaciology (VAW), the WSL Institute for Snow and Avalanche Research SLF, the University of Applied Sciences and Arts of Southern Switzerland (SUPSI) through their Institute of Earth Sciences, the University of Lausanne through the Institute of Earth Surface Dynamics, the University of Innsbruck through the Institute of Informatics, and the Geography Departments of the Universities of Fribourg and Zurich. The Swiss Permafrost Monitoring Network is financially supported by MeteoSwiss, in the framework of GCOS Switzerland, the Federal Office for the Environment FOEN and the Swiss Academy of Sciences SCNAT.

References

Bast, A., Kenner, R., and Phillips, M. 2024. Short-term cooling, drying, and deceleration of an ice-rich rock glacier. *The Cryosphere,* 18, 3141–3158, doi.org/10.5194/tc-18-3141-2024.

Cicoira, A., Marcer, M., Gärtner-Roer, I., Bodin, X., Arenson, L.U., and Vieli, A. 2021. A general theory of rock glacier creep based on in-situ and remote sensing observations. *Permafrost and Periglacial Processes,* 32, 139–153, doi.org/10.1002/ppp.2090.

Davies, M.C.R., Hamza, O., and Harris, C. 2001. The effect of rise in mean annual temperature on the stability of rock slopes containing ice-filled discontinuities. *Permafrost and Periglacial Processes,* 12, 137–144, doi.org/10.1002/ppp.378.

Fehlmann, M., Mani, P., and Stoffel, M. 2016. Der Einfluss des Klimas auf Steinschlag im periglazialen Prozessbereich der Alpen. *FAN Herbstkurs 2016*, 25–31.

Fischer, L., Purves, R.S., Huggel, C., Noetzli, J., and Haeberli, W. 2012. On the influence of topographic, geological and cryospheric factors on rock avalanches and rockfalls in high-mountain areas. *Natural Hazards and Earth System Sciences,* 12, 241–254, doi.org/10.5194/nhess-12-241-2012.

Gruber, S., and Haeberli, W. 2007. Permafrost in steep bedrock slopes and its temperature-related destabilization following climate change. *Journal of Geophysical Research,* 112, DOI: 10.1029/2006JF000547.

Haberkorn, A., Zweifel, B., Techel, F., Marty, C., and Stucki, T. 2025. *Schnee und Lawinen in den Schweizer Alpen, hydrologisches Jahr 2024/25*, Swiss Federal Institute for Forest, Snow and Landscape Research, WSL, doi.org/10.55419/wsl:36046.

Hasler, A., Gruber, S., Font, M., and Dubois, A. 2011. Advective Heat Transport in Frozen Rock Clefts: Conceptual Model, Laboratory Experiments and Numerical Simulation. *Permafrost and Periglacial Processes,* 22, 378–389, doi.org/10.1002/ppp.737.

Hoelzle, M., Hauck, C., Mathys, T., Noetzli, J., Pellet, C., and Scherler, M. 2022. Long-term energy balance measurements at three different mountain permafrost sites in the Swiss Alps. *Earth System Science Data,* 14, 1531–1547, doi.org/10.5194/essd-14-1531-2022.

Irrgang, A.M., Isaksen, K., Noetzli, J., Schoeneich, Philippe, Shiklomanov, N., Cable, W.L., Pellet, C., Coppa, G., Merlone, A., Luo, D., Portnov, A., and Zhao, L. 2024. Measurement of permafrost. In *World Meteorological Organisation. Guide to Instruments and Methods of Observation Volume II (WMO-No.8) – Measurements of Cryospheric Variables*. Geneva, Switzerland, 99–148, doi.org/10.59327/WMO/CIMO/2.

Jacquemart, M., Weber, S., Chiarle, M., Chmiel, M., Cicoira, A., Corona, C., Eckert, N., Gaume, J., Giacona, F., Hirschberg, J., Kaitna, R., Magnin, F., Mayer, S., Moos, C., Van Herwijnen, A., and Stoffel, M. 2024. Detecting the impact of climate change on alpine mass movements in observational records from the European Alps. *Earth-Science Reviews,* 258, 104886, doi.org/10.1016/j.earscirev.2024.104886.

Kellerer-Pirklbauer, A., Bodin, X., Delaloye, R., Lambiel, C., Gärtner-Roer, I., Bonnefoy-Demongeot, M., Carturan, L., Damm, B., Eulenstein, J., Fischer, A., Hartl, L., Ikeda, A., Kaufmann, V., Krainer, K., Matsuoka, N., Morra Di Cella, U., Noetzli, J., Seppi, R., Scapozza, C., Schoeneich, P., Stocker-Waldhuber, M., Thibert, E., and Zumiani, M. 2024. Acceleration and interannual variability of creep rates in mountain permafrost landforms

(rock glacier velocities) in the European Alps in 1995–2022. *Environmental Research Letters,* 19, 034022, doi.org/10.1088/1748-9326/ad25a4.

Kellerer-Pirklbauer, A., Bodin, X., Delaloye, R., Lambiel, C., Gärtner-Roer, I., Damm, B., Ikeda, A., Kaufmann, V., Krainer, K., Seppi, R., Scapozza, C., Stocker-Waldhuber, M., and Thibert, E. 2026. Rock glacier velocity monitored by annual in-situ geodetic surveys: Long-term challenges, solutions and suggestions. *Geomorphology,* 495, 110117, doi.org/10.1016/j.geomorph.2025.110117.

Krautblatter, M., Funk, D., and Günzel, F.K. 2013. Why permafrost rocks become unstable: a rock-ice-mechanical model in time and space. *Earth Surface Processes and Landforms,* 38, 876–887, doi.org/10.1002/esp.3374.

Mamot, P., Weber, S., Eppinger, S., and Krautblatter, M. 2021. A temperature-dependent mechanical model to assess the stability of degrading permafrost rock slopes. *Earth Surface Dynamics,* 1125–1151.

Mellor, M. 1973. Mechanical properties of rocks at low temperatures. In *Proceedings*. 2nd International Conference on Permafrost. Yakutsk, 334–344.

MeteoSwiss 2026. Klimabulletin Jahr 2025. 14 pp., Zurich.

MeteoSchweiz 2025. Klimareport 2024. Bundesamt für Meteorologie und Klimatologie MeteoSchweiz, Zürich. 100 pp.

Mollaret, C., Hilbich, C., Pellet, C., Flores-Orozco, A., Delaloye, R., and Hauck, C. 2019. Mountain permafrost degradation documented through a network of permanent electrical resistivity tomography sites. *The Cryosphere* 13, 2557–2578, doi.org/10.5194/tc-13-2557-2019

Noetzli, J., Arenson, L.U., Bast, A., Beutel, J., Delaloye, R., Farinotti, D., Gruber, S., Gubler, H., Haeberli, W., Hasler, A., Hauck, C., Hiller, M., Hoelzle, M., Lambiel, C., Pellet, C., Springman, S.M., Vonder Muehll, D., and Phillips, M. 2021. Best Practice for Measuring Permafrost Temperature in Boreholes Based on the Experience in the Swiss Alps. *Frontiers in Earth Science* 9, 607875, DOI: 10.3389/feart.2021.607875

Noetzli, J., Hoelzle, M., and Haeberli, W. 2003. Mountain permafrost and recent Alpine rock-fall events: a GIS-based approach to determine critical factors. In *8th International Conference on Permafrost*. 8th International Conference on Permafrost. Zurich, Switzerland, 827–832.

Noetzli, J., Isaksen, K., Barnett, J., Christiansen, H., Delaloye, R., Etzelmuller, B., Farinotti, D., Gallemann, T., Guglielmin, M., Hauck, C., Hilbich, C., Hoelzle, M., Lambiel, C., Magnin, F., Oliva, M., Paro, L., Pogliotti, P., Riedl, C., Schoeneich, P., Valt, M., Vieli, A., and Phillips, M. 2024. Enhanced warming of European mountain permafrost in the early 21st century. *Nature Communications*, doi.org/10.1038/s41467-024-54831-9

Noetzli, J., Peter, A., Hählen, N., and Phillips, M. 2025. Verborgenes Eis in den Schweizer Alpen: Der Permafrost taut immer schneller. In *Forum für Wissen 2025: Extremes (WSL Berichte 164)*. Forum für Wissen 2025: Extremes. Swiss Federal Institute for Forest, Snow and Landscape Research, WSL, 35–47, doi.org/10.55419/wsl:39741

Offer, M., Weber, S., Krautblatter, M., Hartmeyer, I., and Keuschnig, M. 2025. Pressurised water flow in fractured permafrost rocks revealed by borehole temperature, electrical resistivity tomography, and piezometric pressure. *The Cryosphere* 19, 485–506, doi.org/10.5194/tc-19-485-2025

PERMOS 2019. *Permafrost in Switzerland 2014/2015 to 2017/2018*, Fribourg: Cryospheric Commission of the Swiss Academy of Sciences.

PERMOS 2025. *Swiss Permafrost Bulletin 2024*, Fribourg and Davos: Swiss Permafrost Monitoring Network PERMOS.

Roer, I., Haeberli, W., Avian, M., Kaufmann, V., Delaloye, R., Lambiel, C., and Kääb, A. 2008. Observations and considerations on destabilizing active rock glaciers in the European Alps. In *9th International Conference on Permafrost*. 9th International Conference on Permafrost. Fairbanks, US, 1505–1510.

Saibene, G., Gärtner-Roer, I., Beutel, J., and Vieli, A. 2026. Multi-annual and seasonal patterns of Murtèl rock glacier borehole deformation, environmental controls and implications for kinematic monitoring. *The Cryosphere,* 20, 3511–3532, doi.org/10.5194/tc-20-3511-2026

Staub, B., Hasler, A., Noetzli, J., and Delaloye, R. 2017. Gap-Filling Algorithm for Ground Surface Temperature Data Measured in Permafrost and Periglacial Environments. *Permafrost and Periglacial Processes,* 28, 275–285, doi.org/10.1002/ppp.1913

Staub, B., Lambiel, C., and Delaloye, R. 2016. Rock glacier creep as a thermally-driven phenomenon: A decade of inter-annual observation from the Swiss Alps. In *9th International Conference on Permafrost*. 9th International Conference on Permafrost. Potsdam, Germany, 96–97.

Streletskiy, D., Noetzli, J., Smith, S.L., Vieira, G., Schoeneich, P., Hrbacek, F., and Irrgang, A.M. 2021. Strategy and Implementation Plan for the Global Terrestrial Network for Permafrost (GTN-P) 2021–2024, doi.org/10.5281/ZENODO.6075468.

Streletskiy, D., Noetzli, J., Smith, S.L., Vieira, G., Schoeneich, Philippe, Hrbacek, F., and Irrgang, A.M. 2022. Measurement Recommendations and Guidelines for the Global Terrestrial Network for Permafrost (GTN-P), doi.org/10.5281/ZENODO.5973079.

Wirz, V., Beutel, J., Gruber, S., Gubler, S., and Purves, R.S. 2014. Estimating velocity from noisy GPS data for investigating the temporal variability of slope movements. *Natural Hazards and Earth System Sciences,* 14, 2503–2520, doi.org/10.5194/nhess-14-2503-2014.

WMO 2022. *2022 GCOS ECVs Requirements*, Geneva, Switzerland: World Meteorological Organization.

WMO 2017. *WMO Guidelines on the Calculation of Climate Normals*, Geneva: World Meteorological Organization.